The basic helix-loop-helix transcription factor TCF4 recruits the Mediator Complex to activate gonadal genes and drive ovarian development

O'Neil EV, Dupont SM, Singh R, & Capel B*.

Department of Cell Biology, Duke University School of Medicine, Durham NC 27710

*__Correspondence:__ Department of Cell Biology, Duke University School of Medicine. E-mail: blanche.capel@duke.edu

Key words: gonad, development, TCF4

Abstract

The bipotential gonad is the precursor organ to both the ovary and testis and develops as part of the embryonic urogenital system. In mice, gonadogenesis initiates around embryonic day 9.5 (E9.5), when coelomic epithelial (CE) cells overlaying the mesonephric ducts proliferate and acquire competence to differentiate into the somatic cell types of the embryonic gonad, the pre-supporting cell (Sertoli cells in the testis and granulosa cells in the ovary) and the interstitial cell lineages. While some transcription factors that drive gonadal cell fate are known, we found that basic helix-loop-helix (bHLH) binding sites are highly represented upstream of granulosa and interstitial genes. We investigated the bHLH Transcription Factor 4 (TCF4), which is expressed in GATA4+ somatic cells in both sexes prior to sex determination, maintained in ovarian pre-supporting cells and interstitial cells of both sexes, but silenced specifically in male pre-supporting cells. In a *Tcf4*$^{STOP/STOP}$ mutant mouse model that lacks the TCF4 DNA-binding domain, we found that the marker of Sertoli fate, SOX9, was higher in Sertoli cells, while markers of granulosa and interstitial fate (FOXL2 and NR2F2) were reduced and the supporting to interstitial cell ratio was altered in XX *Tcf4*$^{STOP/STOP}$ ovaries. We found that TCF4 binds the Mediator complex and chromatin remodelers to regulate expression of *Jun* and other genes in early somatic cells. Collectively, these results support the working hypothesis that TCF4 regulates a gonadal program that primes the gonad towards a female fate but is specifically silenced in male supporting cells as the testis pathway diverges.

Significant Findings

- bHLH binding sites are more abundant in genes involved in sex-determination than SOX9 or FOXL2 sites, and are 1.5 times more common upstream of granulosa than Sertoli genes.
- TCF4 is a Class I bHLH factor that is expressed in early gonadal progenitors, but silenced in Sertoli cells.
- Loss of the TCF4 binding domain results in higher levels of SOX9, suggesting that TCF4 antagonizes the Sertoli pathway.
- Loss of TCF4 binding domain reduces levels of FOXL2 and NR2F2 and leads to defects in ovary development.
- TCF4 binds with all proteins in the Mediator complex to alter the transcriptional/epigenetic landscape which may explain how it functions on target genes such as Jun.
- Our findings identify *Tcf4* as a potential upstream factor that skews the bipotential supporting cell lineage towards a granulosa cell fate.

42 **Introduction**

43 Differentiation of the bipotential gonad into either a testis or an ovary is a crucial process with
44 implications for adult reproductive function. In mice, the gonad first forms from epithelial cells on the
45 coelomic surface of the mesonephros around embryonic day 9.5 (E9.5) [1-4]. At this stage, the somatic
46 cells of the XX and XY gonad are bipotential, with virtually identical gene expression and high
47 expression of a common set of gonadal genes including *Wt1, Sf1, Gata4,* and *Lhx9* [5-14].

48 Sex determination is the process through which the gonad commits to a testis or ovary fate. The testis
49 pathway is initiated by the expression of the Y-chromosome gene *Sry* in a subset of gonadal precursor
50 cells between E10.5 and E12.5 [15, 16]. *Sry* activates the transcription factor *Sox9,* and SOX9 up-
51 regulates a gene expression network that drives differentiation of these cells into Sertoli cells, the
52 testicular supporting cell lineage [17-25]. Differentiation of XX somatic cells into the ovarian granulosa
53 supporting cell fate is associated with expression of an alternate gene regulatory network that includes
54 *Wnt4, Foxl2,* and *Rspo1* [26-30]. In contrast to the male pathway, the upstream factors that drive initial
55 granulosa cell commitment are unclear [31]. This remains a substantial gap in the sex determination
56 field.

57 An analysis of transcription factor (TF) binding motifs in gonadal cells showed enrichment of basic helix-
58 loop-helix (bHLH) binding sites upstream of granulosa genes (Garcia-Moreno, unpublished data). bHLH
59 proteins are a broad class of TFs that regulate differentiation of cells in many different tissues, including
60 brain and muscle [32-34]. On a molecular level, bHLH TFs typically form homodimers or heterodimers
61 and recognize E-box binding domains (CANNTG) [35, 36]. Of note, the class I bHLH factors, such as
62 MyoD, Twist, and TCF4, are broadly expressed across tissues and are generally associated with
63 transcriptional activation of target genes [37]. In *C. elegans,* the expression of different combinations
64 of class I bHLH TF underly the specification of the sexually dimorphic somatic cell types in the gonad
65 [38]. Whether bHLH factors have a role in sex determination in mammals has not been explored.

66 In the present study, we investigated whether the class I bHLH factor TCF4 plays a biological role in
67 granulosa cell specification. Our results suggest that TCF4 recruits the Mediator complex to activate
68 gonadal genes in both sexes during early gonadogenesis. While the expression of TCF4 is maintained
69 in interstitial lineages in both XX and XY gonads, TCF4 expression is specifically silenced in XY Sertoli
70 cells, whereas TCF4 is maintained in granulosa cells where it binds with FOXL2 and promotes the
71 female pathway. We suggest a working model in which TCF4 binds in a large activation complex to
72 prime the bipotential pre-supporting cell towards a granulosa cell fate in early gonad development.

73

Results

bHLH binding sites are ubiquitous in up- and down-regulated genes in XY and XX gonads.

To determine whether bHLH TFs might play a role in sex determination, we identified genes that were significantly ($P < 0.05$) up- or down-regulated (≥ 1.15-fold) between E11.5 and E13.5 in the supporting and interstitial cell lineages of XY and XX gonads using a transcriptome dataset from the lab (Supplemental Table 1) [5]. In supporting cells, 43% of the genes that were up-regulated in XX gonads contained HLH binding sites, compared to 29% of the genes that increased in XY supporting cells (Figure 1A). Meanwhile, HLH binding sites were present in 47% of the genes that were down-regulated in XX supporting cells, and in 50% of the genes that decreased in XY supporting cells. Surprisingly, we found that bHLH binding sites were more frequent in the promoter region of the top one hundred most up- or down-regulated genes in both XX and XY supporting cells compared to SOX and FOX TF binding sites (Figure 1A).

Within the interstitial cell population, HLH binding sites were present in the promoter region of 53% and 46% of up-regulated genes in XY and XX cells. Additionally, HLH binding sites were present upstream of 57% and 64% of down-regulated interstitial genes in the XY and XX gonad, respectively (Figure 1B).

Many HLH transcription factors are expressed within the early gonad (Figure 1C lists representative examples). The Class I bHLH factors *Tcf4* and *Tcf12,* which are associated with gene activation, are highly expressed in both supporting and interstitial cells (Figure 1C). Unlike *Tcf12*, *Tcf4* shows a strong down-regulation in the XY supporting cell lineage. The Class II bHLH TFs are also associated with gene activation but are either specific to the interstitial lineage (*Tcf21*) or generally expressed at lower levels than the Class I bHLH factors. Class V bHLH factors, including *Id1, Id2, Id3,* and *Bhlhe41,* are also highly expressed in the gonad but are associated with gene repression. Given the high expression levels and the activating role of TCF4, along with its significant sexually dimorphic expression pattern, we focused on investigating the role of this bHLH factor in early gonad development.

The bHLH transcription factor 4, TCF4, is highly expressed in the early gonad and down-regulated in SOX9-expressing cells.

As a role for TCF4 in gonad development has not been previously investigated, we sought to first characterize TCF4's localization in the gonad across gonadogenesis. Using immunostaining (IF), we found that TCF4 was present in the coelomic epithelium and in the broad domain of GATA4+ expressing gonadal cells in XY gonads at E10.75, just prior to sex determination (Figure 2A). At E11.5, expression of TCF4 was excluded from SOX9-expressing cells, but was maintained in XY interstitial cells that were negative for SOX9 (Figure 2B). By E12.5, TCF4 expression became restricted to the interstitial

compartment of the testis (Figure 2C), where it co-localized with the interstitial markers, VCAM and NR2F2 (Supplemental Figure 1A). This expression pattern held through E18.5, near the time of birth (Supplemental Figure 1B).

In XX gonads, TCF4 was co-expressed in GATA4+ gonadal cells at E10.75, as in the XY gonads (Figure 2D). However, while TCF4 expression was excluded from Sertoli progenitor cells in the testis, its expression was maintained in both supporting (RUNX1+) and interstitial (NR2F2+) cell types in the developing ovary (Figure 2E). By E18.5, TCF4 was highly enriched in the interstitial lineage, as in the testis, but TCF4 maintained colocalization with granulosa cell markers (Supplemental Figure 1C). Collectively, TCF4 is rapidly down-regulated in Sertoli cell progenitors, but retained in granulosa progenitors and enriched in the interstitial populations of both ovaries and testes.

Inactivation of the *Tcf4* HLH-DNA binding domain leads to dimorphic effects on the sex determination transcription factors SOX9 and FOXL2.

To understand how loss of T*cf4* affects gonad differentiation *in vivo*, we acquired a knock-out-first mutant mouse line carrying a loxP-P2A-GFP-STOP-loxP cassette in intron 17 of the *Tcf4* gene that produces a truncated form of TCF4-GFP lacking the DNA binding domain (Supplemental Figure 2A) [39]. We confirmed the presence of truncated TCF4 by western blot in protein extracts from gonads and limbs of $Tcf4^{STOP/+}$ and $Tcf4^{+/+}$ fetuses (Supplemental Figure 2B). Offspring homozygous for this disruption of *Tcf4* die a few days post-birth, which restricted our analysis of mutants to fetal stages. Mutant $Tcf4^{STOP/+}$ studs were crossed with $Tcf4^{STOP/+}$ dams, and $Tcf4^{+/+}$ and $Tcf4^{STOP/STOP}$ littermates were collected for downstream analysis.

First, we performed immunostaining to determine if general gonad development was disrupted by *Tcf4* inactivation. XY wildtype $Tcf4^{+/+}$ (n = 3) and mutant $Tcf4^{STOP/STOP}$ (n = 6) littermates showed relatively normal development of the testis, with organization of germ cells into sex cords surrounded by SOX9+ Sertoli cells (Figure 3A). Additionally, HSD3B1+ interstitial cells were present by E15.5, suggesting that interstitial cell types differentiated normally. In XX $Tcf4^{+/+}$ (n = 5) and $Tcf4^{STOP/STOP}$ (n = 5) fetuses, ovary development also progressed relatively normally, with the appearance and organization of FOXL2+ lined ovigerous cords (Figure 3B). However, some $Tcf4^{STOP/STOP}$ mutant ovaries had pockets of FOXL2+ granulosa cells lacking germ cells, suggesting that there could be disruption to ovarian organization in these mutants (Supplemental Figure 3A).

Since bHLH factors specify gonadal cell types and regulate sex determination in invertebrate species [38], we used FACS analysis to test whether loss of TCF4 alters the proportions of supporting and interstitial cells in E15.5 testes and ovaries. Gonad pairs from single fetuses were dissociated, fixed, and stained for markers for supporting cells (SOX9 in XY or FOXL2 in XX) or interstitial cells (NR2F2).

139 Use of FACS analysis allowed us to measure cell numbers and protein abundance using fluorescent
140 readings on a single-cell level. The proportions, ratios, and geometric fluorescence values of *Tcf4*$^{+/+}$
141 and *Tcf4*$^{STOP/STOP}$ gonads are listed in Supplemental Table 2.

142 XY *Tcf4*$^{STOP/STOP}$ mutant gonads (n = 3 XY gonad pairs over 3 litters) had similar proportions of
143 supporting and interstitial cells relative to wildtype *Tcf4*$^{+/+}$ XY gonads (n = 2 XY over 2 litters). However,
144 there was higher expression of SOX9 protein on a per-cell basis in Sertoli cells of *Tcf4*$^{STOP/STOP}$ mutants
145 (n = 10,000 cells per gonad pair, 3 gonad pairs over 3 litters) compared to *Tcf4*$^{+/+}$ littermates (n = 10,000
146 cells per gonad pair, 2 gonad pairs over 2 litters) ($P < 0.05$). There was no difference in levels of the
147 interstitial transcription factor, NR2F2, between wildtype and mutant gonads (Figure 3C).

148 Closer analysis of cell types in the ovary on the BD LSRFortessa™ Analyzer showed that mutant
149 *Tcf4*$^{STOP/STOP}$ ovaries (n = 10,000 cells per gonad pair, 4 gonad pairs over 3 litters) had a greater
150 supporting to interstitial cell ratio relative to XX *Tcf4*$^{+/+}$ wildtype littermates (n = 10,000 cells per gonad
151 pair, 2 gonad pairs over 2 litters). Further, we observed decreases in the average level of both FOXL2
152 and NR2F2 ($P < 0.05$) protein on a per-cell basis relative to wildtype *Tcf4*$^{+/+}$ ovaries (Figure 3D).

153 **Across both sexes, TCF4 recruits the Mediator Complex and other core transcriptional**
154 **machinery to regulate gene expression.**

155 Given the effects of TCF4 inactivation on ovarian development, we sought to further investigate TCF4's
156 function at E12.5 by characterizing binding partners and gene targets around the time of pre-supporting
157 cell commitment to the granulosa cell fate. Using the Nr5a1-GFP line, which labels both supporting and
158 interstitial cells at E12.5 [5, 40], we used FACS to isolate cells, immunoprecipitated TCF4, and
159 performed mass spectrometry (MS) (Figure 4A) (Supplemental Table 3A, B, and C). Binding partners
160 of TCF4 were defined as proteins that showed at least a 1.5-fold difference between the TCF4 IP and
161 IgG IP in each sex. In total, 2,215 proteins co-precipitated with TCF4 in dissociated XX gonadal cells,
162 and 3,130 proteins immunoprecipitated in dissociated XY cells as defined by a significant enrichment
163 ($P = 0.05$, rounded to two decimal places) relative to the IgG control IP. Of these, 1,774 proteins co-
164 precipitated with TCF4 in both XX and XY gonads (Figure 4B). Notably, TCF4 itself was enriched in the
165 TCF4 IP of both XX ($P = 0.05$) and XY cells ($P = 0.04$). The majority of TCF4 binding partners common
166 to both XX and XY gonads were not differentially abundant by sex (96%) and the HLH factor TCF21,
167 an interstitial-specific bHLH TF [41], immunoprecipitated with TCF4 in both XX and XY cells. Shared
168 TCF4 binding partners in both XX and XY cells were enriched in factors involved in positive regulation
169 of transcription (Figure 4C). Many key regulators of basal transcriptional processes co-precipitated with
170 TCF4, including all 24 of the Mediator complex proteins, as well as several classes of epigenetic
171 regulators, co-activators, transcription factors, and the RNA polymerase holoenzyme (Figure 4D). We

172 independently confirmed the presence of one core Mediator protein, Mediator 8, via western blot
173 analysis of a TCF4 pulldown (Figure 4E). While most proteins precipitated with TCF4 in both XY and
174 XX cells, there were also sex-specific TCF4 binders (Figure 4F). Most notably, the core transcription
175 factor, FOXL2, which has well established roles as a crucial regulator of granulosa cell identity, co-
176 precipitated with TCF4 in XX cells.

177 **TCF4 regulates gonadal genes and the transcription factor *Jun* in the ovary.**

178 Finally, ChIP-sequencing was performed using chromatin from either XX or XY *Nr5a*1-GFP cells at
179 E12.5 to identify TCF4 targets and determine if TCF4 directly regulates genes in the granulosa network.
180 Reads were aligned to the mm10 genome assembly, and peaks were called using MACS2 software
181 (Supplemental Table 4). Next, stringent filtration steps were imposed on the data; peaks were filtered
182 out if they had a Q-value < 7 or did not overlap within 1kb across all three sexed replicates (Figure 5A).
183 While this significantly reduced the number of TCF4 targets, it enhanced the robustness of the results
184 and minimized potential biases. In total, 96 peaks and 92 genes were identified across all three XX
185 samples and 16 peaks and 9 genes were identified in XY samples (Figure 5B) (Supplemental Table 4).

186 Given that TCF4 inactivation negatively impacted ovary development, we focused on XX target genes
187 for downstream validation. TCF4 target genes were enriched for processes in regulation of transcription
188 and RNA metabolism (Figure 5C). TCF4 targets unique to XX cells included *Cwc22,* a splicing protein,
189 and *Nfyc* and *Jun,* two transcription factors (Figure 5D). We measured the expression of the XX ChIP
190 target genes *Cwc22, Nfyc*, and *Jun* in the *Tcf4*$^{STOP/STOP}$ mutant gonads relative to *Tcf4*$^{+/+}$ wildtype
191 gonads. While the TCF4 putative targets *Cwc22* and *Nfyc* were not affected in mutants, we observed
192 that expression of *Jun* as well as the granulosa-specific transcription factor *Runx1* were significantly
193 reduced in *Tcf4*$^{STOP/STOP}$ mutant ovaries compared to wildtype *Tcf4*$^{+/+}$ ovaries ($P < 0.05$) (Figure 5E). In
194 contrast, the expression of *Jun* - which was not identified as a TCF4 target in XY cells - and *Runx1*
195 were not dysregulated in *Tcf4*$^{+/+}$ mutant testes relative to *Tcf4*$^{+/+}$ wildtype testes.

196 Although TCF4 regulates *Jun* expression in the ovary, it is unclear whether *Jun* plays a role in ovary
197 development. Transcriptome data and single-cell RNA sequencing show that *Jun* expression becomes
198 higher in the granulosa lineage than in the Sertoli cell lineage shortly after sex determination [5, 7].
199 Consistent with this, *Jun* was more highly expressed in *Tcf4*$^{+/+}$ ovaries than *Tcf4*$^{+/+}$ testes at E15.5
200 (Supplemental Figure 3B). However, JUN must be activated by phosphorylation (P-JUN) to work as a
201 transcription factor – a process that occurs downstream of signaling cascades such as WNT signaling,
202 which plays a pivotal role in ovary development. Thus, we measured P-JUN in whole embryonic ovaries
203 and testes at E12.5 and in XX FACS-sorted *Nr5a1-GFP* gonadal cells across gonad development. We
204 observed that activated P-JUN is more abundant in whole XX gonads compared to XY gonads at E12.5,

205 and that P-JUN is present in Nr5a1-GFP XX somatic gonadal cells across sex determination (from
206 E11.5 to E13.5) (Figure 5F). These results suggest that TCF4 promotes *Jun* expression, and that JUN
207 activation is elevated in XX gonads during ovary development.

208

209 **Discussion**

210 Commitment of the somatic gonad cells to the testicular Sertoli or ovarian granulosa lineage is the first
211 essential step in gonad differentiation. In XY fetuses, *Sry* expression activates transcriptional changes
212 that lead to Sertoli cell fate commitment and development of a testis [5, 7, 20, 42]. In contrast, the
213 upstream regulators driving the granulosa gene regulatory network and *Foxl2* expression in XX cells
214 remain unclear.

215 Across various studies, a group of genes essential for the formation of the bipotential gonad has
216 emerged, including *Nr5a1, Gata4, Wt1, Lhx9,* and *Emx2 [8-10, 12-14].* To search for a common element
217 in the regulation of these genes, we performed an investigation of TF binding sites found upstream of
218 early regulators of gonad differentiation. Binding sites for bHLH TFs were enriched upstream of core
219 gonadal genes, and were 1.5 times more common in genes associated with the ovary pathway than in
220 genes associated with the testis pathway [9, 10, 12, 14].

221 Of the many bHLH factors expressed in gonadal cells, we chose to investigate whether TCF4, which
222 has a known role in gene activation [43-45], plays a role in ovary development. TCF4 is highly
223 expressed in gonadal somatic cells before and during sex determination. However, TCF4 expression
224 is lost in SOX9-expressing cells, a pattern we would predict for a driver of ovarian fate.

225 To test whether TCF4 is involved in directing gonadal fate, we obtained a mutant mouse model for *Tcf4*
226 in which the binding domain is disrupted, but the rest of the protein, including the AD domains that
227 recruit p300 and transcriptional machinery, remain intact [16, 46]. In XY mutant gonads, the loss of
228 TCF4 did not lead to any obvious disruptions in testis development. Instead, we observed higher
229 expression of SOX9 in Sertoli cells. The fact that SOX9 binds upstream of *Tcf4* [47] and that loss of
230 TCF4 led to elevation of SOX9 expression, suggests an antagonistic relationship between SOX9 and
231 TCF4. In future studies, over-expression of TCF4 in SRY/SOX9-expressing Sertoli cells could
232 determine whether TCF4 is inhibitory to Sertoli cell fate.

233 In XX wildtype gonads, TCF4 expression is maintained in granulosa cells in the ovary with highest
234 abundance in the ovarian stroma. In XX *Tcf4* mutant gonads, we saw decreased expression of both the
235 granulosa marker FOXL2 and the ovarian stromal marker, NR2F2 at the single-cell level. Surprisingly,
236 the ratio of granulosa cells to stromal cells was increased in mutants, despite lower levels of FOXL2.

237 Further, defects in patterning and germ cell population were evident in some regions of mutant ovaries.
238 These stronger effects are consistent with the hypothesis that TCF4 positively regulates the ovarian
239 pathway.

240 To better understand how TCF4 functions in the gonad, we performed a MS analysis at E12.5 to identify
241 TCF binding partners in XX and XY gonads. Based on mass spec analysis, binding partners identified
242 in both XX and XY gonads included proteins associated with the Mediator Complex, the RNA
243 polymerase complexes for initiation and elongation, epigenetic regulators, and transcription factors,
244 such as FOXL2. These TCF4 binding partners were also reported in a paper showing that TCF4 binds
245 with and recruits the Mediator complex to super enhancers to regulate neural stem cell differentiation
246 [45]. If TCF4 plays a similar role in the gonad, it may bind to and open genes that establish gonadal
247 fate and set the gonad on an ovary developmental pathway. Consistent with this, a key regulator of the
248 ovarian pathway, FOXL2, was one of a handful of sex-specific binding partners in XX gonads. We
249 speculate that TCF4 works in conjunction with other TF binding partners such as FOXL2 and TCF21,
250 to specify granulosa and interstitial cell identity, respectively [37, 41, 48].

251 If TCF4 acts as a master regulator of gonadal genes, it is unclear why the phenotype in both XX and
252 XY gonads is not more severe. This could be because of the complexity of the Mediator Complex in
253 which loss of a single factor has a small impact, or, alternatively, because the *Tcf4* mutation leaves
254 some functions of the TCF4 protein intact. We favor the latter interpretation, which needs further study.

255 If an effort to identify other upstream regulators of granulosa cell identity previously not recognized, we
256 performed a TCF4 ChIP-sequencing analysis on E12.5 XX and XY gonads. Using stringent methods
257 to confirm binding sites in XX gonads, we identified *Jun*, a transcription factor that is dysregulated in
258 *Tcf4*$^{STOP/STOP}$ mutant ovaries and known to be activated downstream of WNT signaling through the
259 planar cell polarity pathway [49-51]. Our data show that TCF4 promotes *Jun* expression, which is
260 preferentially activated in the embryonic ovary relative to the testis at E12.5. These findings suggest
261 that TCF4 may enhance the availability of JUN as a key mediator of WNT-driven signaling during ovary
262 development.

263 In conclusion, we hypothesize that *Tcf4* is silenced in Sertoli cells to permit their differentiation in
264 response to *Sry* expression. Our data suggest that TCF4 recruits the Mediator complex to specific
265 chromatin regions to maintain the progenitor state of other somatic gonadal cells and partners with
266 proteins such as FOXL2 and TCF21 to regulate expression of granulosa and stromal factors and
267 promote ovary differentiation (Figure 6). Many other bHLH proteins are expressed in the gonad, and
268 further investigation of this interesting class of TFs is warranted.

269

Materials & Methods

Mouse strains and lines. All mice were housed in accordance with the National Institutes of Health guidelines, and experimental procedures were approved by the Duke University Medical Center Institutional Animal Care and Use Committee. For wildtype matings, CD-1 mice were obtained from Jackson Laboratories. The Tg(*Nr5a1-GFP)* (*Sf1-eGFP)* mice have been previously described [40]. The Tg(*Runx1-EGFP)*E1184Gsat/mmucd (*Runx1-eGFP)* mice were a gift from Humphrey Yao (MMRRC 010771-UCD) [52]. The *Tcf4*$^{STOP/+}$ mutant mouse line was a gift from Ben Philpot at UNC where they have been previously characterized [39, 53], and was maintained on a C57BL/6J (B6) background in our colony.

Timed matings. To obtain embryos at specific embryonic stages, females were placed in timed mating cages with studs. Female mice were checked daily for the presence of a vaginal plug, which was considered embryonic day 0.5. Female CD-1 mice were used for all experiments except those involving *Tcf4*$^{STOP/+}$ *mice*. For *Tcf4*$^{STOP/+}$ matings, *Tcf4*$^{STOP/+}$ B6 studs were crossed with *Tcf4*$^{STOP/+}$ B6 females.

Organ collection and genotyping. Gonad-mesonephric complexes were microdissected into PBS and used for downstream applications. Tail somites were counted to ensure mice were at the appropriate developmental stage. Tails or limbs were recovered from each fetus and digested in 150 mM NaOH at 95ºC for 15 minutes and neutralized with 1M Tris HCl (pH 7.4) for genotyping. Fetuses were sexed by genotyping for the *Utx* and *Uty* genes using the following three primers (5'→3'): UTX F1: TCATGTCCATCAGGTGATGG, UTY F2: CAATGTGGACCATGACATTG, UTX/Y R: ATGGACACAGACATTGATGG. Mice from the *Tcf4*$^{STOP/+}$ breeding scheme were genotyped for the wildtype allele (primer sequences 5' → 3' F: GCACTTCAGGGATCGCTTA, R: CCGCCCTAATTGTTCAAAGAG) or transgenic knock-in allele (primer sequences 5' → 3': F: GCTGATCCGGAACCCTTAAGC, with the TCF4 WT R primer). PCR conditions have been previously reported [53, 54]. In the case of *Nr5a1-GFP* mice, fluorescent signal was strong enough to observe with the NIGHTSEA fluorescence detection system on the dissection microscope (NIGHTSEA, Lexington, MA), bypassing the need for genotyping.

Whole mount Immunofluorescence. Embryonic gonads were fixed for 1 hour at room temperature (RT) or overnight (O/N) at 4ºC in 4% paraformaldehyde while rocking. Samples were rinsed 3 times in PBS and then passed through an increasing methanol gradient in PBS (25%, 50%, 75%, 100%). Gonads were stored in 100% methanol O/N or longer, as needed. Samples were rehydrated stepwise into PBS and rinsed 3 times in PBS. Late-stage gonads (E15.5) were incubated in 2% Triton X-100 in PBS for 1 hour at RT to increase permeabilization. Early and late-stage gonads were then incubated in blocking

303 buffer (0.1% Triton X-100 for E10.5-E13.5 or 1% Triton X-100 for E15.5 and later, with 3% BSA, and
304 10% fetal bovine serum or horse serum [HS] in PBS) for 1 hour. Tissue was incubated with primary
305 antibody in blocking solution O/N. Antibody details and concentrations are listed in Table 1. The
306 following day gonads were rinsed in either 0.1% (E10.5-E14.5) or 1% Triton X-100 (E15.5 and later) in
307 PBS and incubated with secondary antibodies (1:500) in blocking buffer O/N. Gonads were rinsed 3
308 times for 10 minutes in PBS and then mounted in DABCO mounting media. Images were captured with
309 a Leica TCS SP8 confocal microscope using the associated Leica software (Leica, Wetzlar Germany).
310 Images were processed using FIJI (ImageJ).

311 *Mapping HLH, SOX, FOX, and COUP binding sites.* HLH motif file was generated for the E-box motif
312 (CANNTG) using the "seq2profile" command from HOMER. HLH sites genome wide were identified
313 using the "scanMotifGenomeWide" tool against the mm9 genome [55]. The resulting bed file from this
314 motif scan, as well as bed files from SOX9 and FOXL2 ChIP-seq studies [47, 56], were processed using
315 the tool "annotatePeaks" to identify nearest gene transcription start sites to each genomic location
316 present in the bed files. Next, gene lists unique to XX and XY supporting and interstitial cells were
317 filtered by their fold-change between E11.5 and E13.5. Genes that showed a 1.15-fold change and that
318 were statistically significant ($P < 0.05$) were defined as 'Increasing' or 'Decreasing' in the supporting
319 and interstitial genes and output as a csv file (Supplemental Table 1). Annotated bed files were
320 converted to csv and uploaded to R studio alongside the gene lists. Gene lists and motif/ChIP sites
321 were compared for overlap using the function "inner_join" based on Gene Symbol. HLH binding sites
322 were searched for within 1 kilobase of the gene of interest.

323 *Fluorescence Activated Cell Sorting (FACS) Analysis.* For cell analysis of E15.5 *Tcf4*$^{+/+}$ or *Tcf4*$^{STOP/STOP}$
324 gonads, gonad pairs from single fetuses were digested in TrypLE (Gibco, Thermo Fisher, Waltham MA)
325 with 0.1% collagenase for 10 minutes at 37ºC. TrypLE was removed from samples and samples were
326 then resuspended in 3% BSA in PBS and filtered through a 50-um filter. Samples were spun down at
327 600 g for 10 minutes at 4ºC and then fixed in 4% PFA with 0.1% Triton X-100. After a 10-minute
328 incubation, samples were spun down again at 600 g for 10 minutes at 4ºC. Samples were left in 3%
329 BSA in PBS at 4ºC for up to ten days before primary antibody staining. Cells were recovered, spun
330 down at 600g for 10 minutes at 4ºC, and then incubated in blocking buffer (10% HS with 0.1% Triton
331 X-100 in PBS) O/N with an antibody to mark interstitial cells (NR2F2) or supporting cells (SOX9/FOXL2
332 antibody depending on the sex of the sample) (Antibody details in Table 1). The following day samples
333 were spun down at 600 g for 10 minutes at 4ºC and placed in blocking buffer with secondary antibody
334 (Donkey anti-Mouse Cy3, donkey anti-rabbit AF647, or donkey anti-goat AF647) for 1 hour at RT.
335 Samples were spun down and rinsed in 3% BSA in PBS twice before analysis. For FACS analysis,
336 wildtype and mutant gonad suspensions were run on an BD LSRFortessa™ Analyzer in a single

337 session. The area of the forward side scatter (FSC-A) and side scatter area (SSC-A) were plotted to
338 isolate cells and remove debris, and the FSC-A and FSC-H were plotted to obtain single cells. Gating
339 conditions were established using unstained gonad cells, and single fluorophore controls (AF657 and
340 Cy3). Voltage settings were as follows: SSC 246, FSC 360, APC 571, PE 505. Next, 5,000 cells from
341 gonad pairs of individual, genotyped *Tcf4*$^{WT/WT}$ *and Tcf4*$^{STOP/STOP}$ fetuses were recorded. Gating was set
342 at a signal of > $10^{2.5}$ for the 647 fluorophore and > $10^{3.1}$ for the Cy3 fluorophore. Cells with fluorescence
343 signal greater than these gating values were identified as 'supporting' or 'interstitial' cells. The ratio of
344 supporting: interstitial cells was then calculated and compared between wildtype and mutant conditions
345 using a two-tailed t-test. The geometric mean, which gives the average fluorescence on a single-cell
346 level in heterogenous populations, was also determined and compared between wildtype and mutant
347 conditions using a two-tailed t-test.

348 *Cell sorting.* For cell sorting of *Nr5a1-GFP* gonads at E12.5, fetuses were sexed by PCR, and the
349 gonads were dissected, pooled by sex, and dissociated for 10 minutes in TrypLE at 37ºC. After
350 digestion, TryPLE was carefully removed, and gonads were resuspended in 10% HS in PBS. The cell
351 suspensions were filtered through a 50-micron filter and sorted on either a BD FACSAria or Astrios Cell
352 Sorter. GFP expression was used to sort somatic cell types, with gating set using a GFP-negative
353 control sample by a Duke Flow Cytometry Core specialist. Cells were recovered and prepared in one
354 of two ways for downstream analysis. For downstream IP-MS and western blot analysis, samples were
355 spun down at 3500 g for 10 minutes at 4ºC, snap-frozen, and stored at -80ºC. For ChIP-sequencing,
356 cells were first centrifuged at 500 g for 10 minutes at 4ºC, rinsed twice in PBS +/+, and fixed for 10
357 minutes at RT in freshly prepared 1% formaldehyde. Cross-linking was quenched with 2.5 M glycine
358 and incubated for 5 minutes at 4ºC. Cells were then rinsed twice in ice cold PBS and lysed in cell lysis
359 buffer (10 mM Tris HCl pH 7.5, 10 mM NaCl, 3 mM $MgCl_2$, 0.5% NP-40, 1 mM DTT, 1 mM PMSF, 1x
360 Protease inhibitor) for 10 minutes at 4ºC. Nuclear pellets were spun down at 500 g for 5 minutes at 4ºC,
361 the supernatant was removed, and samples were stored at -80ºC for later pooling

362 *IP-MS.* Frozen sorted somatic gonadal cells were pooled into three replicates of 4 million cells (± 10%).
363 Cell pellets were lysed in a Pierce™ IP Lysis Buffer (Thermo Fisher) containing 1 mM PMSF and 1x
364 Halt™ Protease Inhibitor Cocktail (Thermo Fisher), incubated on ice for 30 minutes, and centrifuged at
365 14,000 g for 10 minutes at 4ºC. Meanwhile, 50 µl of Protein G Dynabeads (Invitrogen, Waltham MA)
366 were rinsed 3 times in PBS with 0.05% Tween-20 using a magnet bar. Beads were suspended in 237.5
367 µl of Conjugation buffer (20 m HEPES in PBS), and 5 µg of IgG or TCF4 antibody (Abcam, NCI-R159-
368 6) was crosslinked to the beads using 12.5 µl of 100 mM BS3. Beads were gently vortexed and
369 incubated for 30 minutes in crosslinking buffer. After incubation, beads were resuspended in 250 µl of
370 Conjugation buffer and quenched with 12.5 µl of 1 M Tris HCl (pH 7.5). Beads were incubated for 15

371 minutes at RT and rinsed 3 times in PBS with 0.05% Tween-20. The extracted protein was then split
372 between IgG or TCF4-conjugated beads and incubated O/N on an end-over-end rotator at 4ºC. The
373 following day beads were rinsed in dilution buffer (10 mM Tris HCl pH 7.5 with 150 mM NaCl and 0.5
374 mM EDTA), dilution buffer with 1% Triton X-100, dilution buffer with 1% Triton X-100 and 360 mM NaCl,
375 and finally in dilution buffer. Proteins were eluted at 80ºC for 10 minutes in 25 mM Tris, 50 mM NaCl,
376 and 1% SDS and submitted to the Duke Proteomics Core for MS analysis.

377 *Quantitative LC-MS.* Samples were spiked with 1 or 2 pmol bovine casein as an internal quality control
378 standard. The samples were brought to a final concentration of 5% SDS and reduced for 15 minutes at
379 80ºC. After reduction, the samples were alkylated with 20 mM iodoacetamide for 30 minutes at RT, then
380 supplemented with 1.2% phosphoric acid and 416 µl of S-Trap (Protifi, Firport NY) binding buffer (90%
381 MeOH/100 mM TEAB). Proteins were trapped on the S-Trap microcartridge, digested with 20 ng/µl of
382 trypsin (Promega, Madison WI) for 1 hour at 47 ºC, and eluted sequentially with 50 mM TEAB, followed
383 by 0.2% formic acid (FA) and 50% aceconitrile/0.2% FA. All samples were lyophilized and resuspended
384 in 1% TFA/2% acetonitrile with 12.5 fmol/µl of yeast alcohol dehydrogenase. A study pool sample was
385 created by combining equal volumes of each sample. Quantitative LC/MS was performed on an EvoSep
386 One UPLC coupled to a Thermo Orbitrap Astral high-resolution, accurate-mass tandem mass
387 spectrometer (Thermo Fisher). Each sample was eluted from the EvoTip onto a 1.5 µm EvoSep 150
388 µm ID x 1 5cm performance EvoSep column using the SPD30 gradient at 55ºC. Data collection on the
389 Orbitrap Astral mass spectrophotometer was performed in a data-independent acquisition (DIA) mode
390 of acquisition with a resolution of 240,000 for full MS scans in the m/z range of 380-980. An HCD
391 collision energy setting of 27% was used for all MS2 scans.

392 *Quantitative Proteomics Data Analysis*. Raw data were imported into Spectronaut (Biognosis, Zurich
393 Switzerland) and individual LC-MS data files were aligned based on the accurate mass and retention
394 time of detected precursor and fragment ions. Relative peptide abundance was measured based on
395 MS2 fragment ions of selected ion chromatograms of the aligned features across all runs. The MS/MS
396 data was searched against a SwissProt M. musculus database and an equal number of reversed-
397 sequence "decoys" for false discovery rate determination. A library free Direct DIA+ approach within
398 Spectronaut was used to perform the database searches. Database search parameters included a fixed
399 modification on Cys (carbamidomethyl), with variable modification on Met (oxidation) and Lys (biotin).
400 Full trypsin enzyme rules were applied, along with 10ppm mass tolerances on precursor ions and
401 20ppm on product ion. Spectral annotation was set at a maximum 1% peptide false discovery rate,
402 based on q-value calculations. Peptide homology was addressed using razor rules, where a peptide
403 that matches to multiple different proteins is exclusively assigned to the protein with the most identified
404 peptides. Protein homology was handled by grouping proteins that had the same set of peptides to

account for their identification. Fold-changes were calculated between the IgG and TCF4 group using a two-tailed heteroscedastic t-test on log2-transformed data. The P-Value was rounded to two decimals points. Proteins were enriched TCF4 binding partners if they met the criteria of being at least 1.5-fold higher than the IgG value with a P-value $\leq$ 0.05.

Western blot analysis. Protein was extracted from *Nr5a1-GFP* cells using Pierce™ RIPA Lysis Buffer (Thermo Fisher) with 1 mM of PMSF and 1x Halt Protease and Phosphatase inhibitor cocktail (Thermo Fisher). Protein isolates from *Nr5a1-Gfp* cells were quantified using a BCA assay. For the western blot, equivalents amount of protein [200,000 sorted cells worth of protein extract for the P-JUN western blot in *Nr5a1-GFP* cells, 20 µg of measured protein extract for the western blot measuring P-JUN and MED8 in whole gonads, or 30 µl of eluant from the IgG or TCF4 IP (approximately half the total eluant from 4 million cell IP reaction split between IgG or TCF4 antibody)] was reduced with 5x Laemmli buffer and 1 mM DTT at 95ºC for 5 minutes. Samples were loaded onto a mini-PROTEAN TGX precast gel (Bio-Rad, Hercules, CA) and proteins were separated via SDS-PAGE at a constant voltage of 100 V for 90 minutes in running buffer (25 mM Tris, 192 mM glycine, 0.1% SDS). Protein was transferred using a Trans-Blot Turbo Transfer System (Bio-Rad), following the Manufacturer's Instructions. Membrane was blocked for 1 hour at 5% milk in 0.1% Tris-Buffered saline with 0.1% Tween-20 (TBST) and incubated O/N with a polyclonal rabbit MED8, monoclonal rabbit P-JUN, or monoclonal rabbit TCF4 antibody. Blot was rinsed three times in 0.1% TBST and then put in blocking buffer with goat anti-rabbit horseradish peroxidase (HRP) conjugated secondary antibody at a 1:10,000 dilution for 1 hour at RT. Blot was rinsed three times in 0.1% TBST and developed in Super Signal West Pico Chemiluminescent Substrate (Thermo Fisher) for 5 minutes before visualization on an Amersham Imager 600. For non-IP western blots, blots were stripped in Restore PLUS Western Blot Stripping buffer for 15 minutes at RT. Blots were blocked for 1 hour in 5% milk in 0.1% TBST again and then either stained with Colloidal Gold Total Protein Stain (Bio-Rad) or incubated with a polyclonal goat anti-GAPDH antibody (1:5,000) O/N. The following day, the blot was rinsed three times in 0.1% TBST and incubated in a donkey anti-goat horseradish peroxidase (HRP) conjugated secondary antibody. Development and imaging were repeated as previously described.

ChIP Sequencing. Nuclear pellets from approximately 1.75 million (± 10%) sorted *Nr5a*1-GFP cells were pooled and placed in a MNase reaction buffer (10mM Tris HCl pH 7.5, 10mM NaCl, 3 mM MgCl2, 1 mM Cacl2, 0.2% NP-40, 1 mM DTT, 1mM PMSF, 1x protease inhibitor). Nuclei were centrifuged at 500 g for 5 minutes at 4ºC and placed in 200 µl of fresh MNAse reaction buffer. Next, 55 units of MNase was added to each tube and nuclear pellets were incubated for 15 minutes at 37ºC with vortexing every five minutes. Enzymatic DNA fragmentation was stopped by adding 20 µl of 0.5 M EDTA. Samples were centrifuged at 9400 g for 10 minutes at 4ºC and placed in 75 µl of ChIP sonication buffer (50 mM

439 Tris HCl pH 7.9, 10 mM EDTA, 1% SDS, 1mM PMSF, 1x protease inhibitor). Samples were left on ice
440 for 10 minutes and 75 µl of ChIP dilution buffer (16.7 mM Tris HCl pH 7.9, 1.1% Triton X-100, 167 mM
441 NaCl, 1.2 mM EDTA, 1 mM PMSF). DNA was sonicated four times for 20 seconds with 30 seconds of
442 rest. Samples were centrifuged at 13000g for 10 minutes at 4ºC. Next, 600 µl of ChIP dilution buffer
443 was added to samples, 2% of the sample volume was collected for input, and 5 µg of TCF4 antibody
444 was added for overnight incubation at 4ºC on an end-over-end rotator. The following day, 15 µl of
445 Dynabeads Protein G magnetic beads were added to each tube. Samples were incubated for two hours
446 on an end-over-end rotator. Using a magnetic bar, the supernatant was removed and beads were
447 sequentially rinsed for 10 minutes in low salt buffer (20 mM Tris HCl pH 7.9, 100 mM NaCl, 2 mM EDTA,
448 0.1% SDS, 1% Triton X-100), high salt buffer (20 mM Tris HCl pH 7.9, 500 mM NaCl, 2 mM EDTA,
449 0.1% SDS, 1% Triton X-100), LiCl Buffer (10 mM Tris HCl pH 7.9, 250 mM LiCl, 1% NP-40, 1%
450 deoxycholate acid, 1 mM EDTA) and TE buffer. Next, 200 µl of elution buffer (1% SDS, 0.1 M $NaHCO_3$)
451 was added and samples were left at 65ºC for 40 minutes to elute DNA. At this point, input DNA was
452 thawed, brought to 200 µl with elution buffer, and processed in parallel with samples. Samples were
453 recovered, 8 µl of 5 M NaCl (per 200 µl of elution buffer) was added to samples, and samples were left
454 at 55ºC overnight to de-crosslink the DNA. The next day, 14 µl of Proteinase K solution was added to
455 each sample (4 µl of 0.5 M EDTA, 8 µl of 1 M Tris HCl pH 6.8, 2 µl of 20 mg/ml Proteinase K) before a
456 2-hour incubation at 55ºC, and DNA was eluted using the Qiagen MinElute on column PCR Purification
457 kit (Qiagen, Hilden, Germany). DNA was eluted in 10 ul of TE buffer.

458 *ChIP sequencing data analysis.* Samples were submitted to BGI Genomics for sequencing and
459 analysis. Briefly, immunoprecipitated DNA was purified and checked for quality using a Fragment
460 Analyzer. Sequencing libraries were prepared by adding ligating sequencing adaptors and sequenced
461 on the DNBSEQ platform to generate 50 bp paired-end reads. After adapter trimming and removal of
462 low-quality reads, an average of approximately 25 million high-quality reads were obtained per sample.
463 Clean reads were aligned to the reference genome mm10 using SOAPaligner/SOAP2 software with
464 two mismatches. Only uniquely mapped reads with a mapping quality score (MAPQ) greater than 20
465 were retained. Peak calling was performed using MACS1.4.2 with a Q-value cutoff of < 0.05 relative to
466 the input control. Individual peak lists were generated for the six replicates (three sexed replicates). We
467 then selected high-confidence peaks (Q-value < 10^-7) and designed a replicate-matching algorithm to
468 only select peaks that were consistently observed across the three sexed replicates. Specifically, we
469 computed clusters of peaks such that each cluster a) contains at least one peak from each replicate,
470 and b) each peak in the cluster is within 1 kb of at least one peak from another replicate. This was
471 achieved by constructing a tri-partite graph across three replicates where nodes are peaks, edges
472 connect cross-replicate peaks within 1 kb and then identifying connected graph sub-components that

span all replicates. Peaks not assigned to any cluster were discarded. The Python implementation of the matching algorithm will be made available to the research community as an open-source package on Github. The peaks called after stringent filtration as well as the peak lists for each individual replicate are listed in Supplementary Table 4. Individual bigWig files are available for download at DOI 10.17605/OSF.IO/H6D2M. Raw FASTQ files will be deposited in GEO and made publicly available upon publication.

qPCR analysis. Tissue was dissected and run through a QiaShredder column in Buffer RLT (Qiagen). RNA was isolated using the MinElute RNA Kit (Qiagen), including an on-column DNAse digestion. The RNA was quantified using a Nanodrop and the purity was assessed using A260/280 values. Next, 50 ng of RNA was reverse-transcribed into cDNA using the Verso cDNA Synthesis kit. Parallel reactions were run without enzyme to assess genomic contamination. Reverse transcription was performed following manufacturers' instructions. Real-time PCR was then performed using a QuantStudio 6 Flex Real-Time System (ThermoFisher) with SsoAdvanced Universal SyberGreen Supermix (BioRad). PCR conditions were: activation, 95°C for 15 min; 40 cycles of 95°C for 15 s; 60°C for 60 s. Primers were synthesized by Integrated DNA Technologies (Primer sequences in Table 2). Technical triplicates were used to generate the cycle threshold for each gene in each sample. Melt curve analysis was performed to verify PCR product specificity. ΔCT values were calculated as the difference between the cycle threshold (CT) of the gene of interest and the housekeeping gene (*Actb)*. The housekeeping gene *Actb* is highly and stably expressed during early gonad development [5, 7]. Statistics were calculated using the ΔCT values. For visualization, fold change was calculated relative to the reference gene. Standard error was calculated by propagating the standard deviations of the gene of interest and housekeeping gene using the formula $SE_{\Delta\Delta CT} = \sqrt{[(SD_GOI/\sqrt{n})^2)+(SD_HK/\sqrt{n})^2]}$. Fold change was plotted as $2^{-\Delta\Delta CT} \pm$ propagated error.

Table 1. Key Resources.

Reagent type (species) or resource	Designation	Source or reference	Identifiers	Additional information
Gene (*M. musculus*)	Transcription factor 4 (Tcf4)	GenBank	MGI:98506	
Strain, strain background (*Mus musculus*)	Crl:CD1(ICR)	Charles River	Strain code: 022	

Reagent type (species) or resource	Designation	Source or reference	Identifiers	Additional information
Strain, strain background (*M. musculus*)	C57BL/6J	Jackson Laboratory	Stock #:000664	
Genetic reagent (*M. musculus*)	Tg(Nr5a1/EGFP)1Klp	PMID:12351700	MGI:5493455	
Genetic reagent (*M. musculus*)	Tg(Tcf4$^{STOP/+}$)	PMID: 32765228		
Antibody	Smooth muscle alpha actin (aSMA) (FITC-conjugated mouse monoclonal)	Sigma-Aldrich	F3777	1:500
Antibody	Endostatin/Collagen 18 (goat polyclonal)	R&D Systems	AF570	1:500
Antibody	FOXL2 (rabbit polyclonal)	Gift from Dagmar Wilhelm		1:250
Antibody	GATA4 (mouse monoclonal $IgG_{2\alpha}$)	Santa Cruz Biotechnology	Sc-25310	1:250
Antibody	GFP (chicken polyclonal)	Abcam	Ab13970	1:1000
Antibody	Phospho-c-Jun (Ser73) (rabbit monoclonal)	CellSignaling Technology	(D47G9)	1:1000
Antibody	Phospho-JUN (Ser73)	Proteintech	4A18	1:1000
Antibody	MED8 (rabbit polyclonal)	Proteintech	12182-1-AP	1:1000
Antibody	NR2F2 (mouse monoclonal $IgG_{2\alpha}$)	Abcam	Ab41859	1:200
Antibody	NR5A2 (goat polyclonal)	Santa Cruz Biotechnology	Sc-21132	1:500
Antibody	SOX9 (goat polyclonal)	R&D Systems	AF3075	1:500
Antibody	TCF4 (rabbit monoclonal)	Abcam	Ab217668	1:500

Reagent type (species) or resource	Designation	Source or reference	Identifiers	Additional information
Antibody	TRA98/GCNA1 (rat monoclonal)	Abcam	Ab82527	1:500
Antibody	AF488 Anti-Mouse (donkey polyclonal)	Jackson ImmunoResearch	715-545-150	1:500
Antibody	AF488 anti-Rat (donkey polyclonal)	Life Technologies	A-21208	1:500
Antibody	AF488 anti-Chicken (donkey polyclonal)	Jackson ImmunoResearch	703-545-155	1:500
Antibody	Cy3 anti-Goat (donkey polyclonal)	Jackson ImmunoResearch	705-165-147	1:500
Antibody	Cy3 anti-Mouse (donkey polyclonal)	Jackson ImmunoResearch	715-165-150	1:500
Antibody	AF647 anti-Rabbit (donkey polyclonal)	Jackson ImmunoResearch	711-605-152	1:500

Table 2. qPCR Primer Sequences.

Gene	Forward/Reverse Sequences	Amplicon Size	Origin of Primers
Cwc22	5' – CCAGAGACAACCCACGCA ATA C - 3'	127 nt	Origene SKU MP202029
	5' – TGGTTCTGGGCTACGATGACC – 3'		
Nfyc	5' – CCAGACACTTGCTACCAATGCC – 3'	118 nt	Origene SKU MP220268
	5' – AGGCATGGT GAC TTG CTG GAT C -3'		
Jun	5' – TGA TCA TCC AGT CCA GCA ATG -3'	85 nt	Galán-Cobo et al. 2015 [57]
	5' – TGC TCG TCG GTC ACG TTC T -3'		
Runx1	5' – CACCGTCTTTACAAATCCGCCAC– 3'	141 nt	Lambert et al. 2024 [58]
	5' – CGCTCGGAAAAGGACAAACTCC - 3'		

Acknowledgments

The authors would like to thank Ben Philpot at UNC Chapel Hill for generously providing the Tcf4$^{STOP/+}$mouse line. The authors thank the past and present members of the Capel Lab for their support, especially Megan Harward for providing animal care and maintenance and Talia Hatkevich for assistance in FACS analysis. Finally, the authors would like to thank Erik Soderblom, Tricia Ho, and Greg Waitt for their technical assistance with mass spec sample analysis and interpretation. The

authors also appreciate the Staff at the Duke Light Microscopy Core Facility and the Duke Cancer Institute Flow Cytometry Shared Resource for their excellent technical support.

Funding Sources

EO, SD, and B.C. are currently supported by a grant from the National Institutes of Health (1R01HD090050-0 to BC).

Author contributions

EVO, SMD, and BC conceptualized and designed research; EVO and BC performed research; EVO, SMD, RH, and BC analyzed data; and EVO and BC wrote the manuscript. All authors edited and approved the final manuscript.

Competing Interests

None declared.

REFERENCES

1. Karl, J. and B. Capel, *Three-dimensional structure of the developing mouse genital ridge.* Philos Trans R Soc Lond B Biol Sci, 1995. **350**(1333): p. 235-42.
2. Karl, J. and B. Capel, *Sertoli cells of the mouse testis originate from the coelomic epithelium.* Dev Biol, 1998. **203**(2): p. 323-33.
3. Upadhyay S, L.J., Zombini L, *The role of the mesonephros in the development of indifferent gonads and ovaries of the mouse.* Annales de biologie animale, biochimie, biophysique, 1979. **19**(4 B): p. 1179-1196.
4. Wartenberg, H., *Human testicular development and the role of the mesonephros in the origin of a dual Sertoli cell system.* Andrologia, 1978. **10**(1): p. 1-21.
5. Jameson, S.A., et al., *Temporal transcriptional profiling of somatic and germ cells reveals biased lineage priming of sexual fate in the fetal mouse gonad.* PLoS Genet, 2012. **8**(3): p. e1002575.
6. Munger, S.C. and B. Capel, *Sex and the circuitry: progress toward a systems-level understanding of vertebrate sex determination.* Wiley Interdiscip Rev Syst Biol Med, 2012. **4**(4): p. 401-12.
7. Stevant, I., et al., *Dissecting Cell Lineage Specification and Sex Fate Determination in Gonadal Somatic Cells Using Single-Cell Transcriptomics.* Cell Rep, 2019. **26**(12): p. 3272-3283 e3.
8. Sasaki, K., et al., *The embryonic ontogeny of the gonadal somatic cells in mice and monkeys.* Cell Rep, 2021. **35**(5): p. 109075.
9. Hu, Y.C., L.M. Okumura, and D.C. Page, *Gata4 is required for formation of the genital ridge in mice.* PLoS Genet, 2013. **9**(7): p. e1003629.
10. Kreidberg, J.A., et al., *WT-1 is required for early kidney development.* Cell, 1993. **74**(4): p. 679-91.
11. Luo, X., Y. Ikeda, and K.L. Parker, *A cell-specific nuclear receptor is essential for adrenal and gonadal development and sexual differentiation.* Cell, 1994. **77**(4): p. 481-90.
12. Miyamoto, N., et al., *Defects of urogenital development in mice lacking Emx2.* Development, 1997. **124**(9): p. 1653-64.
13. Birk, O.S., et al., *The LIM homeobox gene Lhx9 is essential for mouse gonad formation.* Nature, 2000. **403**(6772): p. 909-13.
14. Luo, X., et al., *Steroidogenic factor 1 is the essential transcript of the mouse Ftz-F1 gene.* Mol Endocrinol, 1995. **9**(9): p. 1233-9.
15. Gubbay, J., et al., *A gene mapping to the sex-determining region of the mouse Y chromosome is a member of a novel family of embryonically expressed genes.* Nature, 1990. **346**(6281): p. 245-50.
16. Hiramatsu, R., et al., *A critical time window of Sry action in gonadal sex determination in mice.* Development, 2009. **136**(1): p. 129-38.
17. Colvin, J.S., et al., *Male-to-female sex reversal in mice lacking fibroblast growth factor 9.* Cell, 2001. **104**(6): p. 875-89.
18. Li, Y., M. Zheng, and Y.F. Lau, *The sex-determining factors SRY and SOX9 regulate similar target genes and promote testis cord formation during testicular differentiation.* Cell Rep, 2014. **8**(3): p. 723-33.
19. Morais da Silva, S., et al., *Sox9 expression during gonadal development implies a conserved role for the gene in testis differentiation in mammals and birds.* Nat Genet, 1996. **14**(1): p. 62-8.
20. Sekido, R. and R. Lovell-Badge, *Sex determination involves synergistic action of SRY and SF1 on a specific Sox9 enhancer.* Nature, 2008. **453**(7197): p. 930-4.
21. Bullejos, M. and P. Koopman, *Spatially dynamic expression of Sry in mouse genital ridges.* Dev Dyn, 2001. **221**(2): p. 201-5.
22. Hacker, A., et al., *Expression of Sry, the mouse sex determining gene.* Development, 1995. **121**(6): p. 1603-14.
23. Koopman, P., et al., *Male development of chromosomally female mice transgenic for Sry.* Nature, 1991. **351**(6322): p. 117-21.
24. Sekido, R., et al., *SOX9 is up-regulated by the transient expression of SRY specifically in Sertoli cell precursors.* Dev Biol, 2004. **274**(2): p. 271-9.
25. Moniot, B., et al., *The PGD2 pathway, independently of FGF9, amplifies SOX9 activity in Sertoli cells during male sexual differentiation.* Development, 2009. **136**(11): p. 1813-21.
26. Kim, Y., et al., *Fgf9 and Wnt4 act as antagonistic signals to regulate mammalian sex determination.* PLoS Biol, 2006. **4**(6): p. e187.

27. Ottolenghi, C., et al., *Loss of Wnt4 and Foxl2 leads to female-to-male sex reversal extending to germ cells.* Hum Mol Genet, 2007. **16**(23): p. 2795-804.
28. Tomizuka, K., et al., *R-spondin1 plays an essential role in ovarian development through positively regulating Wnt-4 signaling.* Hum Mol Genet, 2008. **17**(9): p. 1278-91.
29. Parma, P., et al., *R-spondin1 is essential in sex determination, skin differentiation and malignancy.* Nat Genet, 2006. **38**(11): p. 1304-9.
30. Nicol, B., et al., *RUNX1 maintains the identity of the fetal ovary through an interplay with FOXL2.* Nat Commun, 2019. **10**(1): p. 5116.
31. Yao, H.H., *The pathway to femaleness: current knowledge on embryonic development of the ovary.* Mol Cell Endocrinol, 2005. **230**(1-2): p. 87-93.
32. Dennis, D.J., S. Han, and C. Schuurmans, *bHLH transcription factors in neural development, disease, and reprogramming.* Brain Res, 2019. **1705**: p. 48-65.
33. Rudnicki, M.A., et al., *The molecular regulation of muscle stem cell function.* Cold Spring Harb Symp Quant Biol, 2008. **73**: p. 323-31.
34. Schlaeger, T.M., et al., *Decoding hematopoietic specificity in the helix-loop-helix domain of the transcription factor SCL/Tal-1.* Mol Cell Biol, 2004. **24**(17): p. 7491-502.
35. de Martin, X., R. Sodaei, and G. Santpere, *Mechanisms of Binding Specificity among bHLH Transcription Factors.* Int J Mol Sci, 2021. **22**(17).
36. Torres-Machorro, A.L., *Homodimeric and Heterodimeric Interactions among Vertebrate Basic Helix-Loop-Helix Transcription Factors.* Int J Mol Sci, 2021. **22**(23).
37. Wang, L.H. and N.E. Baker, *E Proteins and ID Proteins: Helix-Loop-Helix Partners in Development and Disease.* Dev Cell, 2015. **35**(3): p. 269-80.
38. Sallee, M.D., H.E. Littleford, and I. Greenwald, *A bHLH Code for Sexually Dimorphic Form and Function of the C. elegans Somatic Gonad.* Curr Biol, 2017. **27**(12): p. 1853-1860 e5.
39. Kim, H., et al., *Rescue of behavioral and electrophysiological phenotypes in a Pitt-Hopkins syndrome mouse model by genetic restoration of Tcf4 expression.* Elife, 2022. **11**.
40. Stallings, N.R., et al., *Development of a transgenic green fluorescent protein lineage marker for steroidogenic factor 1.* Mol Endocrinol, 2002. **16**(10): p. 2360-70.
41. Cui, S., et al., *Disrupted gonadogenesis and male-to-female sex reversal in Pod1 knockout mice.* Development, 2004. **131**(16): p. 4095-105.
42. Neirijnck, Y., et al., *Single-cell transcriptomic profiling redefines the origin and specification of early adrenogonadal progenitors.* Cell Rep, 2023. **42**(3): p. 112191.
43. Henthorn, P., M. Kiledjian, and T. Kadesch, *Two distinct transcription factors that bind the immunoglobulin enhancer microE5/kappa 2 motif.* Science, 1990. **247**(4941): p. 467-70.
44. Pscherer, A., et al., *The helix-loop-helix transcription factor SEF-2 regulates the activity of a novel initiator element in the promoter of the human somatostatin receptor II gene.* EMBO J, 1996. **15**(23): p. 6680-90.
45. Quevedo, M., et al., *Mediator complex interaction partners organize the transcriptional network that defines neural stem cells.* Nat Commun, 2019. **10**(1): p. 2669.
46. Bullejos, M. and P. Koopman, *Delayed Sry and Sox9 expression in developing mouse gonads underlies B6-Y(DOM) sex reversal.* Dev Biol, 2005. **278**(2): p. 473-81.
47. Rahmoun, M., et al., *In mammalian foetal testes, SOX9 regulates expression of its target genes by binding to genomic regions with conserved signatures.* Nucleic Acids Res, 2017. **45**(12): p. 7191-7211.
48. Murre, C., et al., *Interactions between heterologous helix-loop-helix proteins generate complexes that bind specifically to a common DNA sequence.* Cell, 1989. **58**(3): p. 537-44.
49. Park, M. and R.T. Moon, *The planar cell-polarity gene stbm regulates cell behaviour and cell fate in vertebrate embryos.* Nat Cell Biol, 2002. **4**(1): p. 20-5.
50. Waudby, C.A., et al., *An intrinsic temporal order of c-JUN N-terminal phosphorylation regulates its activity by orchestrating co-factor recruitment.* Nat Commun, 2022. **13**(1): p. 6133.
51. Smeal, T., et al., *Oncogenic and transcriptional cooperation with Ha-Ras requires phosphorylation of c-Jun on serines 63 and 73.* Nature, 1991. **354**(6353): p. 494-6.
52. Gong, S., et al., *A gene expression atlas of the central nervous system based on bacterial artificial chromosomes.* Nature, 2003. **425**(6961): p. 917-25.

625 53. Kim, H., et al., *Region and Cell Type Distribution of TCF4 in the Postnatal Mouse Brain.* Front Neuroanat, 2020. **14**:
626 p. 42.
627 54. Shpargel, K.B., et al., *KDM6 demethylase independent loss of histone H3 lysine 27 trimethylation during early*
628 *embryonic development.* PLoS Genet, 2014. **10**(8): p. e1004507.
629 55. Heinz, S., et al., *Simple combinations of lineage-determining transcription factors prime cis-regulatory elements*
630 *required for macrophage and B cell identities.* Mol Cell, 2010. **38**(4): p. 576-89.
631 56. Nicol, B., et al., *Genome-wide identification of FOXL2 binding and characterization of FOXL2 feminizing action in*
632 *the fetal gonads.* Hum Mol Genet, 2018. **27**(24): p. 4273-4287.
633 57. Galan-Cobo, A., et al., *Overexpression of AQP3 Modifies the Cell Cycle and the Proliferation Rate of Mammalian*
634 *Cells in Culture.* PLoS One, 2015. **10**(9): p. e0137692.
635 58. Lambert, J., et al., *Network-based prioritization and validation of regulators of vascular smooth muscle cell*
636 *proliferation in disease.* Nat Cardiovasc Res, 2024. **3**(6): p. 714-733.

637
638

639 **Figure Legends.**

640 **Figure 1. Helix-loop-helix transcription factor binding sites are ubiquitous in dynamically**
641 **regulated gonadal genes.** A) In supporting cells, HLH binding motifs are present in the promoter
642 region of 29% and 43% of genes that increase in XY and XX cells, respectively, and 50% and 47% of
643 genes that decrease in XY and XX cells. Among the top 100 most up- and down-regulated genes in
644 these sets, HLH binding sites are more frequent than SOX or FOX binding sites. B) In interstitial cells,
645 HLH binding sites are present in 53% and 46% of genes that increase in XY and XX cells, respectively.
646 HLH binding sites are enriched in the top 100 most up-regulated genes and occur more frequently than
647 SOX or FOX binding sites. Additionally, HLH binding sites are upstream of 57% and 64% of genes that
648 decrease in XY and XX interstitial cells and are present in nearly 75% of the top 100 most down-
649 regulated interstitial genes. C) Basic helix-loop-helix transcription factors show sex- and cell-type
650 specificity in the gonad (Jameson et al. 2012).

651 **Figure 2. Expression of the HLH transcription factor TCF4 is lost in Sertoli cells but maintained**
652 **in granulosa and interstitial cell types.** A) At E10.75, TCF4 co-localizes with GATA4-expressing
653 gonadal cells in XY gonads. B) At E11.5, TCF4 is lost in SOX9-expressing Sertoli cells in the XY testis,
654 (shown with arrows in B' and B'') but is maintained in cells throughout the gonad which are forming sex
655 cords (dotted circle in B' and B''). C) In the XY gonad, TCF4 is restricted to the interstitial cell population
656 (shown with dotted lines in C' and C''). D) in the XX gonad, TCF4 is co-expressed in GATA4-expressing
657 cells. E) By E12.5, TCF4 is expressed in both RUNX1 expressing granulosa cells and NR2F2+
658 interstitial cells. Dashed line highlights the boundary between ovarian supporting cells and interstitial
659 cells. Scale bar represents 100 µm. Microscopy images are stitched together from individual panels.

660 **Figure 3. TCF4 does not disrupt gonad differentiation but does affect expression of master**
661 **regulators of sex determination and cell type ratios in the ovary**. A) Immunofluorescence imaging
662 of wildtype *Tcf4*$^{+/+}$ and mutant *Tcf4*$^{STOP/STOP}$ XY gonads. Images were taken using identical microscope
663 settings. Representative images shown. B) Immunofluorescence imaging of wildtype *Tcf4*$^{+/+}$ and mutant
664 *Tcf4*$^{STOP/STOP}$ XX gonads. Images were taken using identical microscope settings. Representative
665 images shown. Microscopy images are stitched together from individual panels. C) Gonads were
666 digested and run on a cell analyzer. While ratios of supporting: interstitial cell types did not change,
667 SOX9 was more abundant ($P < 0.05$) on a per-cell bases in *Tcf4*$^{STOP/STOP}$ XY gonads (n=3 gonad pairs)
668 relative to *Tcf4*$^{+/+}$ gonads (n=2 gonad pairs). Meanwhile, NR2F2 was not different between samples. D)
669 Mutant ovaries had a higher supporting: interstitial cell ratio ($P < 0.05$). Additionally, FOXL2 and NR2F2
670 were less abundant ($P < 0.05$) on a per-cell bases in *Tcf4*$^{STOP/STOP}$ XX gonads (n = 4 gonad pairs)
671 relative to *Tcf4*$^{+/+}$ gonads (n = 2 gonad pairs).

672 **Figure 4. TCF4 binds core transcriptional regulators including the Mediator complex in both XX**
673 **and XY sorted cells.** A) *Nr5a1-Gfp* cells were sorted, immunoprecipitated for TCF4, and sent for mass
674 spectrometry analysis to identify TCF4 binding partners. B) In total, 1,774 proteins were identified as
675 TCF4 co-binders common to XY and XX cells. C) Proteins bound by TCF4 were enriched for processes
676 such as positive transcription initiation and regulation of transcription, suggesting that TCF4 is a pro-
677 transcriptional regulator in the gonad. D) Several protein complexes were identified in our mass
678 spectrometry dataset in both XY and XX cells. Notably, the Mediator complex, as well as members of
679 transcriptional elongation, the RNA polymerase holoenzyme, the MLL complex, and transcriptional
680 initiation machinery. Proteins organized in a circle are known complex proteins, and lines indicate
681 interactions. E) XY and XX *Nr5a1-Gfp* cells were sorted and western blot was performed to show the
682 presence of Mediator 8 in somatic gonadal cells (20 µg input). Presence of Med8 was also shown in
683 the western blot of IP'd TCF4 from XY cells (2 million cells / IP). **F**) Additionally, TCF4 co-precipitated
684 with sex-specific proteins, including FOXL2, STAT1, and NFYB in XX cells and STAT3, LMX1B, and
685 KDM4A in XY cells. These proteins were associated with translational machinery in XY cells, and
686 metabolic processing in XX cells.

687 **Figure 5. Gene targets of TCF4 include *Jun* and other transcriptional regulators.** A) *Nr5a1-Gfp*
688 cells were sorted and a ChIP-sequencing experiment was performed to identify TCF4 target genes in
689 XX and XY chromatin. B) In total, 92 genes were identified as TCF4 targets in XX cells, while only 9
690 genes were identified in XY cells. C) TCF4 targets were enriched for processes including negative and
691 positive regulation of gene transcription and RNA metabolism. D) TCF4 directly binds to the first exon
692 of the splicing factor, *Cwc22,* the transcription factor, *Nfyc,* and across the gene body of the transcription
693 factor *Jun.* E) *Jun,* a TCF4 ChIP target identified in XX cells, and *Runx1* expression is decreased in
694 *Tcf4*$^{STOP/STOP}$ ovaries relative to *Tcf4*$^{+/+}$ ovaries from wildtype littermates. In contrast, *Jun* was not
695 identified as a TCF4 ChIP target in XY cells and was not dysregulated in *Tcf4*$^{STOP/STOP}$ mutant testes.
696 Gene expression was normalized to the housekeeping gene *Actb.* Expression is displayed as $\log_2$-fold
697 change; statistics were calculated based on ΔCT value comparing wildtype and mutant gonads of the
698 same sex. F) The active, phosphorylated form of JUN (P-JUN) is more abundant in E12.5 ovaries
699 compared to E12.5 testes. By E15.5, P-JUN is less abundant in the embryonic ovary than testis.
700 Additionally, P-JUN is present in sorted XX gonadal *Nr5a1-Gfp* cells across early gonad development
701 (E10.5-E13.5) (approximately 200,000 cells per lane). Total protein stain showed similar loading of
702 protein across the different samples.

703 **Figure 6. Working model for the role of TCF4 in gonad differentiation.** TCF4 drives a gonadal
704 program, likely through recruitment of the Mediator complex and epigenetic factors, that advances

705 ovarian fate and is specifically silenced in Sertoli supporting cells as these pathways diverge. Figure
706 created with Biorender.

707 **Figure S1. Expression of TCF4 is maintained in gonadal granulosa and interstitial cells through**
708 **late gestation.** A) At E12.5, TCF4 co-localizes with VCAM- and NR2F2- expressing interstitial cells in
709 XY gonads. B) At E18.5, TCF4 remains restricted to the testicular interstitial cells and absent in SOX9-
710 expressing Sertoli cells. C) At E18.5, TCF4 is broadly expressed across both granulosa and interstitial
711 cell lineages in the oary. Scale bar represents 100 µm. Microscopy images are stitched together from
712 individual panels.

713 **Figure S2. The *Tcf*^{STOP} allele is unable to bind DNA.** A) The *Tcf*^{STOP} allele introduces a premature
714 STOP codon upstream of the bHLH domain in exon 18. B) Western blot analysis shows that *Tcf*$^{STOP/+}$
715 mice express a truncated form of TCF4 without the bHLH domain that is absent in *Tcf*$^{+/+}$ wildtype
716 littermates.

717 **Figure S3. Minor defects** in *Tcf*$^{STOP/STOP}$ mutant ovaries. A) One *Tcf*$^{STOP/STOP}$ mutant ovary displayed
718 defects in patterning, as germ cells were present in the posterior portion of the ovary (white arrowheads)
719 but were absent in the anterior portion. B) The transcription factor *Jun* is expressed in *Tcf*$^{+/+}$ wildtype
720 testes at about half the level of *Tcf*$^{+/+}$ wildtype ovaries.

Fig1

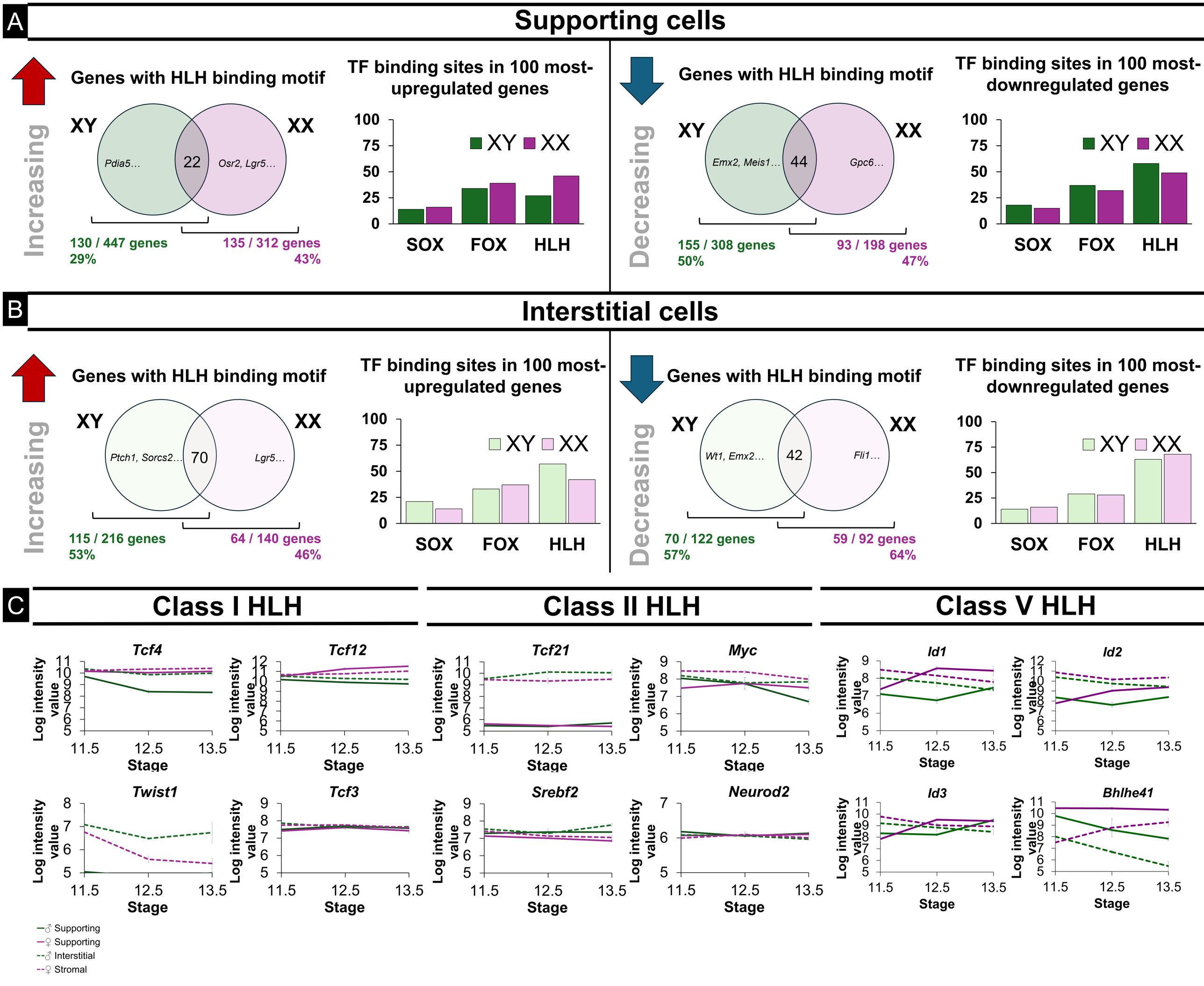
A
Supporting cells
Increasing
Genes with HLH binding motif
XY
XX
Pdia5…
22
Osr2, Lgr5…
130 / 447 genes
29%
135 / 312 genes
43%
TF binding sites in 100 most-upregulated genes
XY
XX
SOX
FOX
HLH
Decreasing
Genes with HLH binding motif
Emx2, Meis1…
44
Gpc6…
155 / 308 genes
50%
93 / 198 genes
47%
TF binding sites in 100 most-downregulated genes
B
Interstitial cells
Increasing
Genes with HLH binding motif
Ptch1, Sorcs2…
70
Lgr5…
115 / 216 genes
53%
64 / 140 genes
46%
TF binding sites in 100 most-upregulated genes
Decreasing
Genes with HLH binding motif
Wt1, Emx2…
42
Fli1…
70 / 122 genes
57%
59 / 92 genes
64%
TF binding sites in 100 most-downregulated genes
C
Class I HLH
Class II HLH
Class V HLH
Tcf4
Tcf12
Tcf21
Myc
Id1
Id2
Twist1
Tcf3
Srebf2
Neurod2
Id3
Bhlhe41
Log intensity value
Stage
♂ Supporting
♀ Supporting
♂ Interstitial
♀ Stromal

Fig2

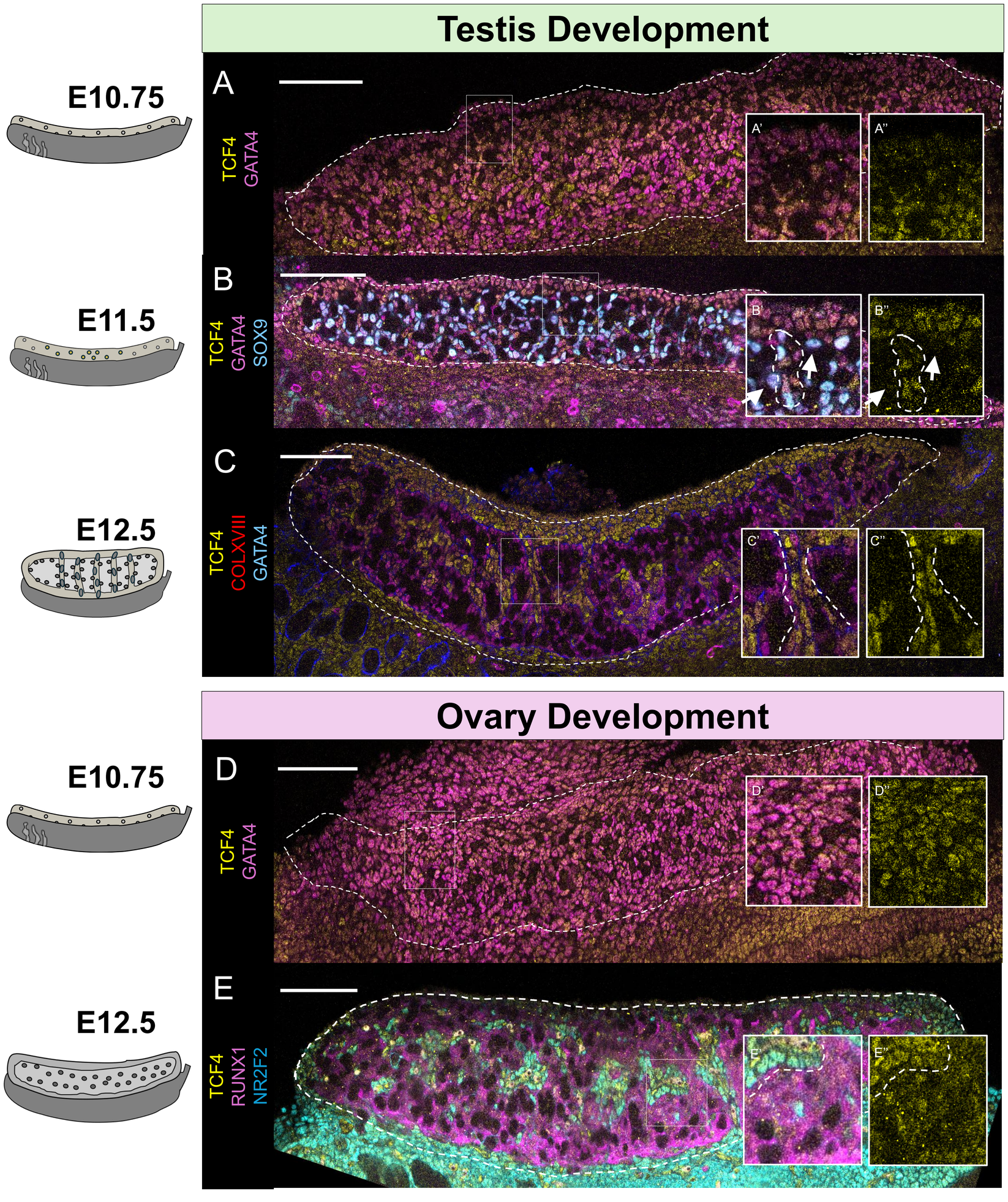
Testis Development
E10.75
A
TCF4
GATA4
A'
A''
E11.5
B
TCF4
GATA4
SOX9
B'
B''
E12.5
C
TCF4
COLXVIII
GATA4
C'
C''
Ovary Development
E10.75
D
TCF4
GATA4
D'
D''
E12.5
E
TCF4
RUNX1
NR2F2
E'
E''

Fig3

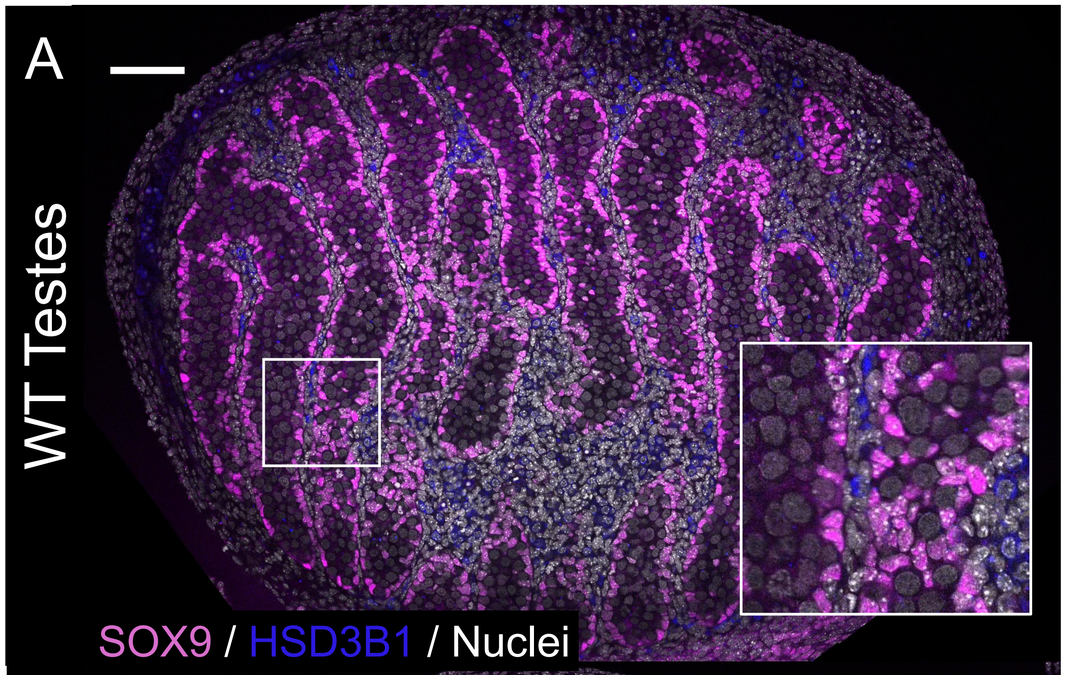
A
WT Testes
SOX9 / HSD3B1 / Nuclei

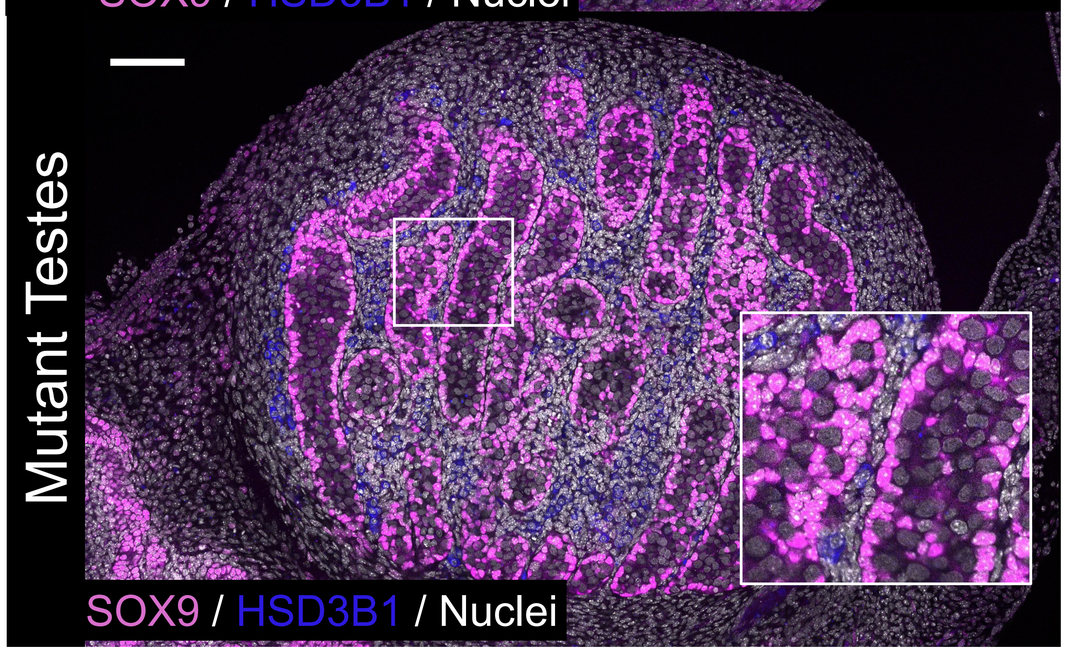
Mutant Testes
SOX9 / HSD3B1 / Nuclei

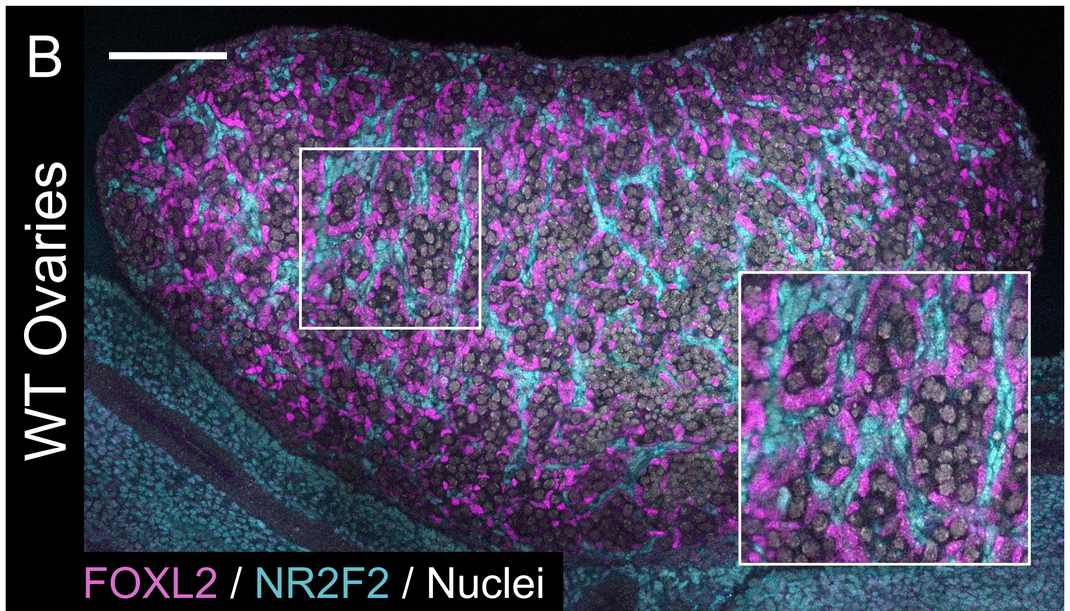
B
WT Ovaries
FOXL2 / NR2F2 / Nuclei

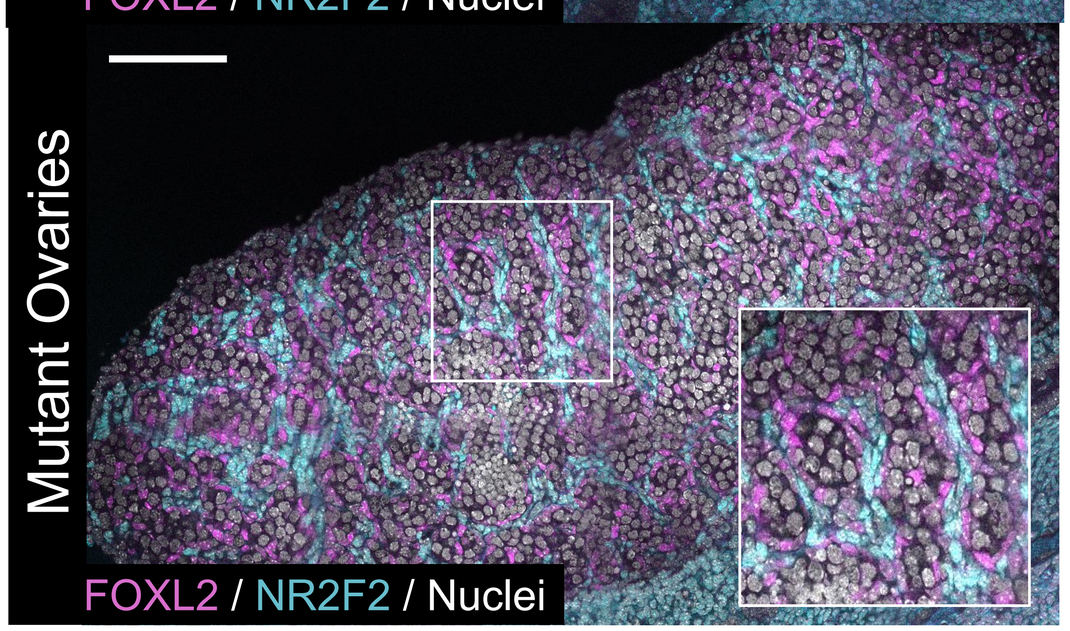
Mutant Ovaries
FOXL2 / NR2F2 / Nuclei

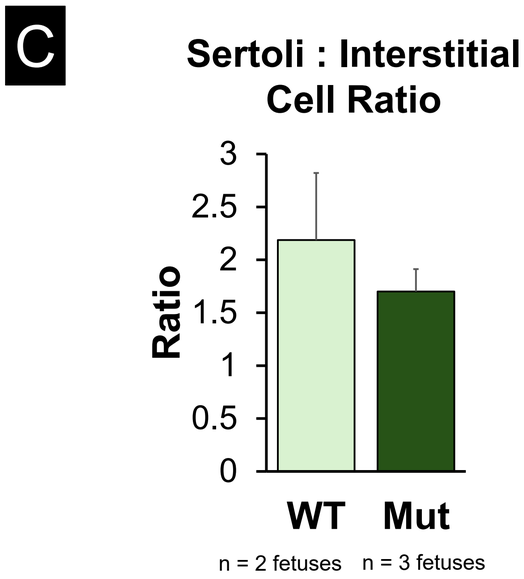
C
Sertoli : Interstitial Cell Ratio
Ratio
3
2.5
2
1.5
1
0.5
0
WT
Mut
n = 2 fetuses
n = 3 fetuses

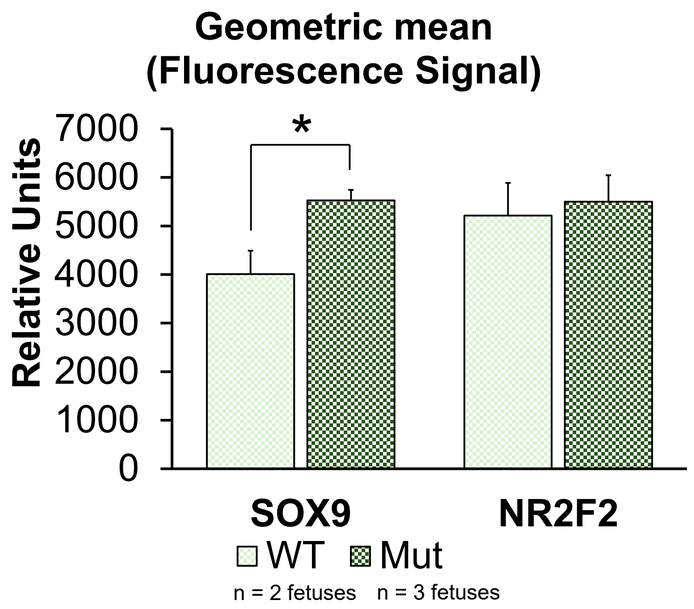
Geometric mean (Fluorescence Signal)
Relative Units
7000
6000
5000
4000
3000
2000
1000
0
*
SOX9
NR2F2
WT
Mut
n = 2 fetuses
n = 3 fetuses

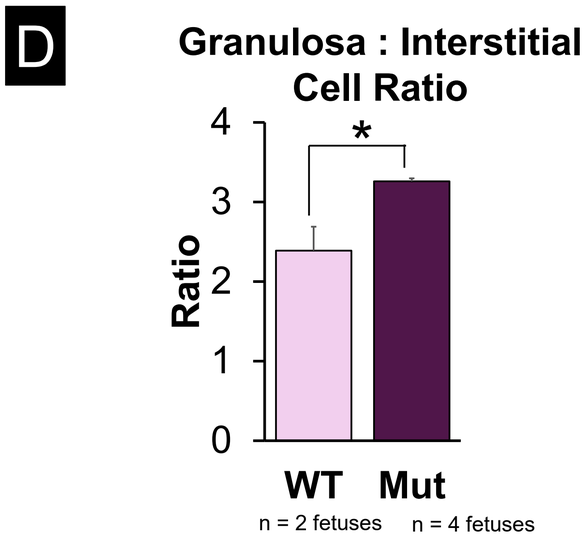
D
Granulosa : Interstitial Cell Ratio
Ratio
4
3
2
1
0
*
WT
Mut
n = 2 fetuses
n = 4 fetuses

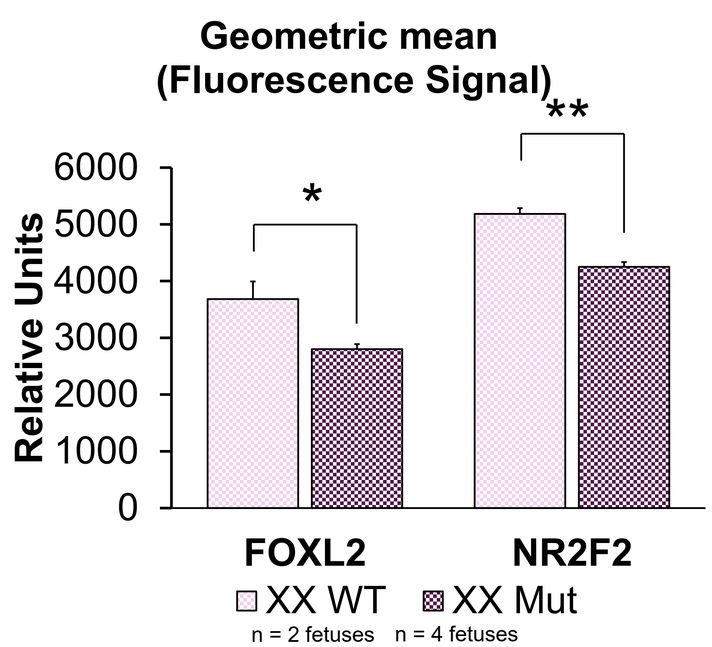
Geometric mean (Fluorescence Signal)
Relative Units
6000
5000
4000
3000
2000
1000
0
*
**
FOXL2
NR2F2
XX WT
XX Mut
n = 2 fetuses
n = 4 fetuses

Fig4

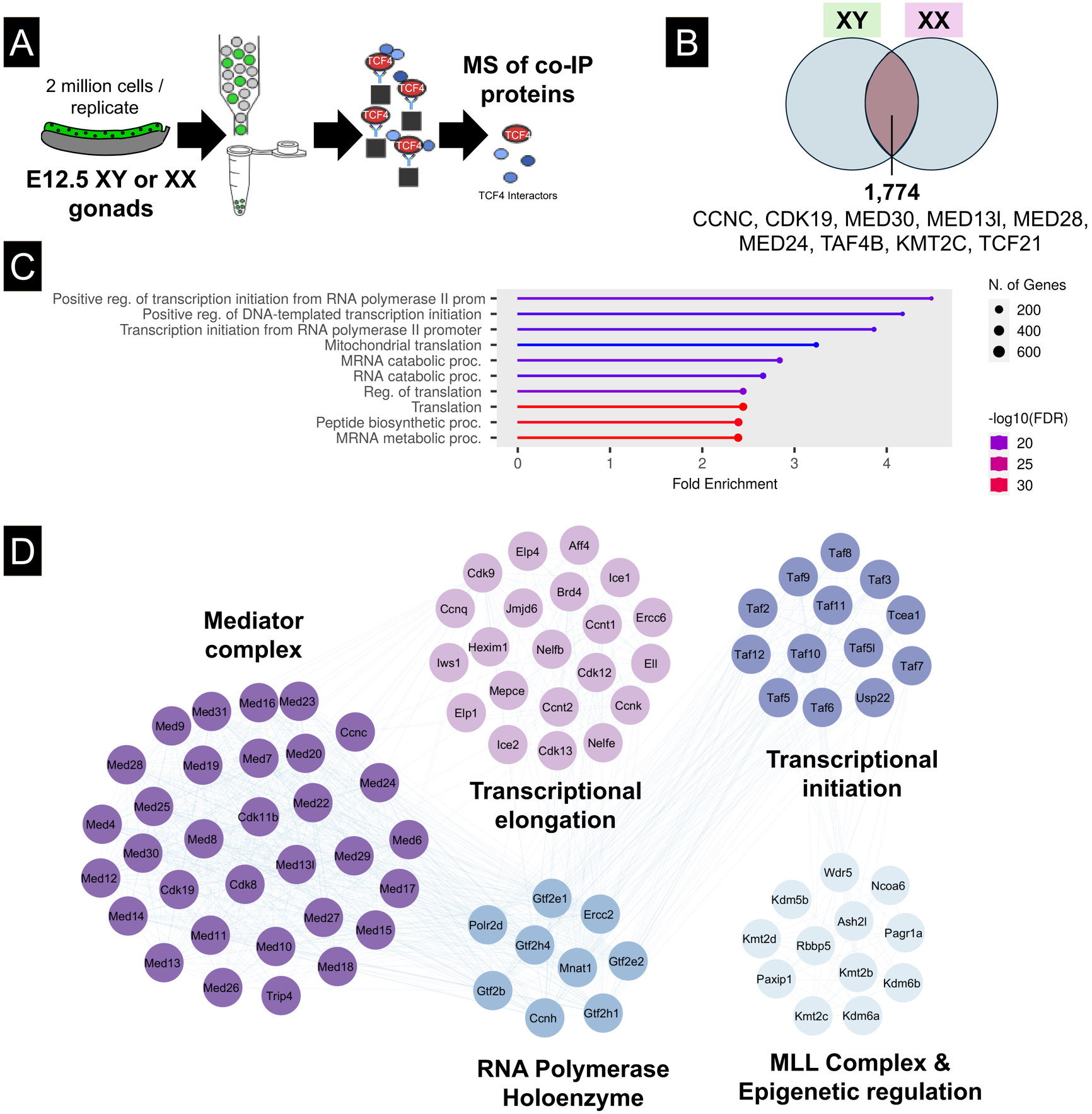
A
2 million cells / replicate
E12.5 XY or XX gonads
TCF4
MS of co-IP proteins
TCF4 Interactors
B
XY
XX
1,774
CCNC, CDK19, MED30, MED13l, MED28, MED24, TAF4B, KMT2C, TCF21
C
Positive reg. of transcription initiation from RNA polymerase II prom
Positive reg. of DNA-templated transcription initiation
Transcription initiation from RNA polymerase II promoter
Mitochondrial translation
MRNA catabolic proc.
RNA catabolic proc.
Reg. of translation
Translation
Peptide biosynthetic proc.
MRNA metabolic proc.
0
1
2
3
4
Fold Enrichment
N. of Genes
200
400
600
-log10(FDR)
20
25
30
D
Mediator complex
Med31
Med16
Med23
Med9
Ccnc
Med28
Med19
Med7
Med20
Med24
Med25
Cdk11b
Med22
Med4
Med8
Med6
Med30
Med13l
Med29
Med12
Cdk19
Cdk8
Med17
Med14
Med27
Med15
Med11
Med10
Med13
Med18
Med26
Trip4
Elp4
Aff4
Cdk9
Ice1
Brd4
Ccnq
Jmjd6
Ccnt1
Ercc6
Hexim1
Nelfb
Iws1
Ell
Cdk12
Mepce
Elp1
Ccnt2
Ccnk
Ice2
Cdk13
Nelfe
Transcriptional elongation
Taf8
Taf9
Taf3
Taf2
Taf11
Tcea1
Taf12
Taf10
Taf5l
Taf7
Taf5
Taf6
Usp22
Transcriptional initiation
Gtf2e1
Ercc2
Polr2d
Gtf2h4
Mnat1
Gtf2e2
Gtf2b
Ccnh
Gtf2h1
RNA Polymerase Holoenzyme
Wdr5
Ncoa6
Kdm5b
Ash2l
Pagr1a
Kmt2d
Rbbp5
Paxip1
Kmt2b
Kdm6b
Kmt2c
Kdm6a
MLL Complex & Epigenetic regulation
E
SF1-GFP+ sorted cells
kDa
XX
XY
35
25
MED8
TCF4-IP
kDa
IgG
TCF4
35
25
MED8
F
XY
XX
STAT3
LMX1B
KDM4A
ZNF710
NFATC4
1,356
441
FOXL2
SP2
STAT1
VP1
NFYB

Fig5

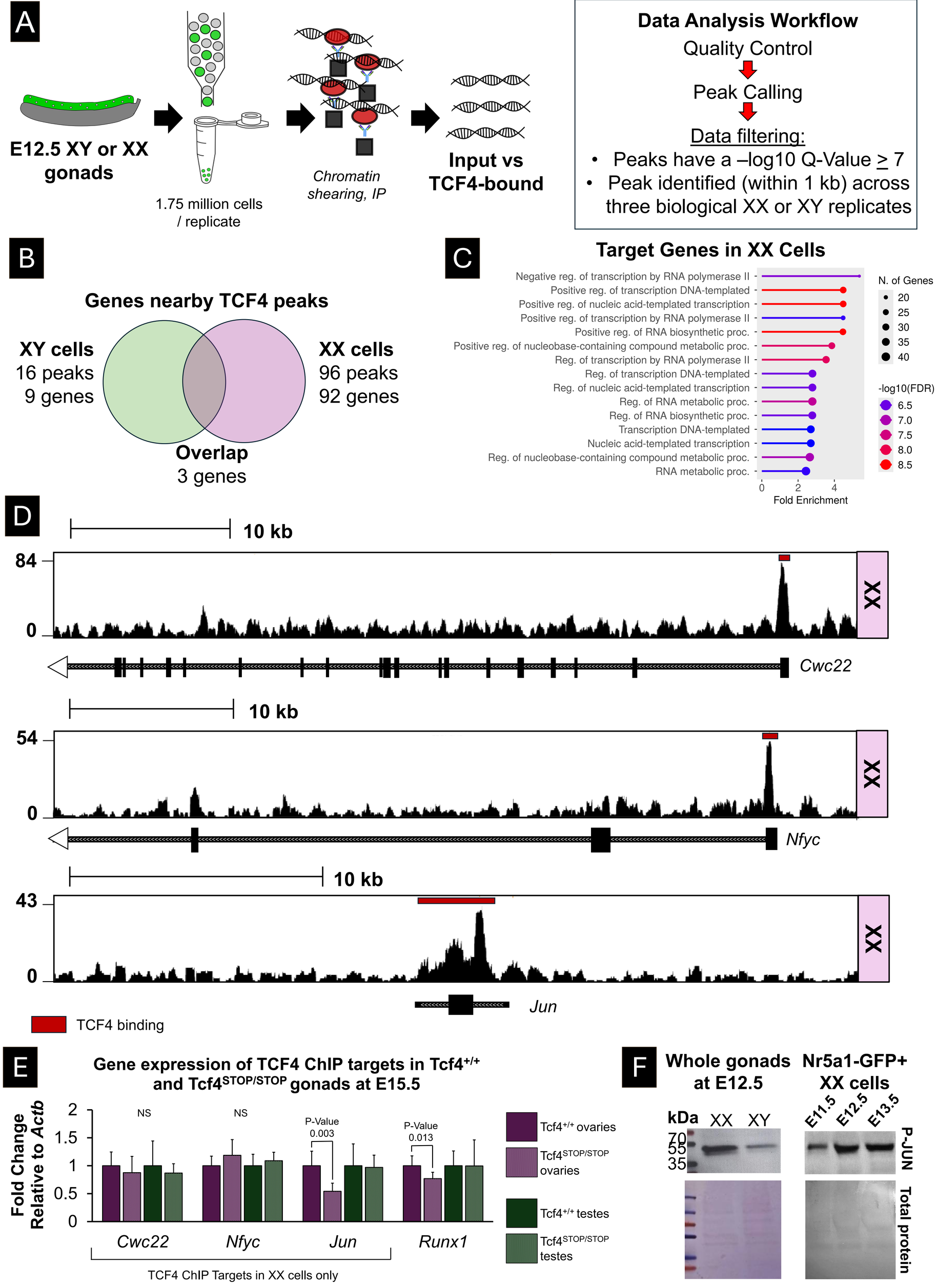
A
E12.5 XY or XX gonads
1.75 million cells / replicate
Chromatin shearing, IP
Input vs TCF4-bound
Data Analysis Workflow
Quality Control
Peak Calling
Data filtering:
• Peaks have a –log10 Q-Value ≥ 7
• Peak identified (within 1 kb) across three biological XX or XY replicates
B
Genes nearby TCF4 peaks
XY cells
16 peaks
9 genes
XX cells
96 peaks
92 genes
Overlap
3 genes
C
Target Genes in XX Cells
Negative reg. of transcription by RNA polymerase II
Positive reg. of transcription DNA-templated
Positive reg. of nucleic acid-templated transcription
Positive reg. of transcription by RNA polymerase II
Positive reg. of RNA biosynthetic proc.
Positive reg. of nucleobase-containing compound metabolic proc.
Reg. of transcription by RNA polymerase II
Reg. of transcription DNA-templated
Reg. of nucleic acid-templated transcription
Reg. of RNA metabolic proc.
Reg. of RNA biosynthetic proc.
Transcription DNA-templated
Nucleic acid-templated transcription
Reg. of nucleobase-containing compound metabolic proc.
RNA metabolic proc.
0
2
4
Fold Enrichment
N. of Genes
20
25
30
35
40
-log10(FDR)
6.5
7.0
7.5
8.0
8.5
D
10 kb
84
0
XX
Cwc22
10 kb
54
0
XX
Nfyc
10 kb
43
0
XX
Jun
TCF4 binding
E
Gene expression of TCF4 ChIP targets in Tcf4+/+ and Tcf4STOP/STOP gonads at E15.5
Fold Change Relative to Actb
2
1.5
1
0.5
0
NS
NS
P-Value 0.003
P-Value 0.013
Cwc22
Nfyc
Jun
Runx1
TCF4 ChIP Targets in XX cells only
Tcf4+/+ ovaries
Tcf4STOP/STOP ovaries
Tcf4+/+ testes
Tcf4STOP/STOP testes
F
Whole gonads at E12.5
Nr5a1-GFP+ XX cells
kDa
XX
XY
70
55
35
E11.5
E12.5
E13.5
P-JUN
Total protein

Fig6

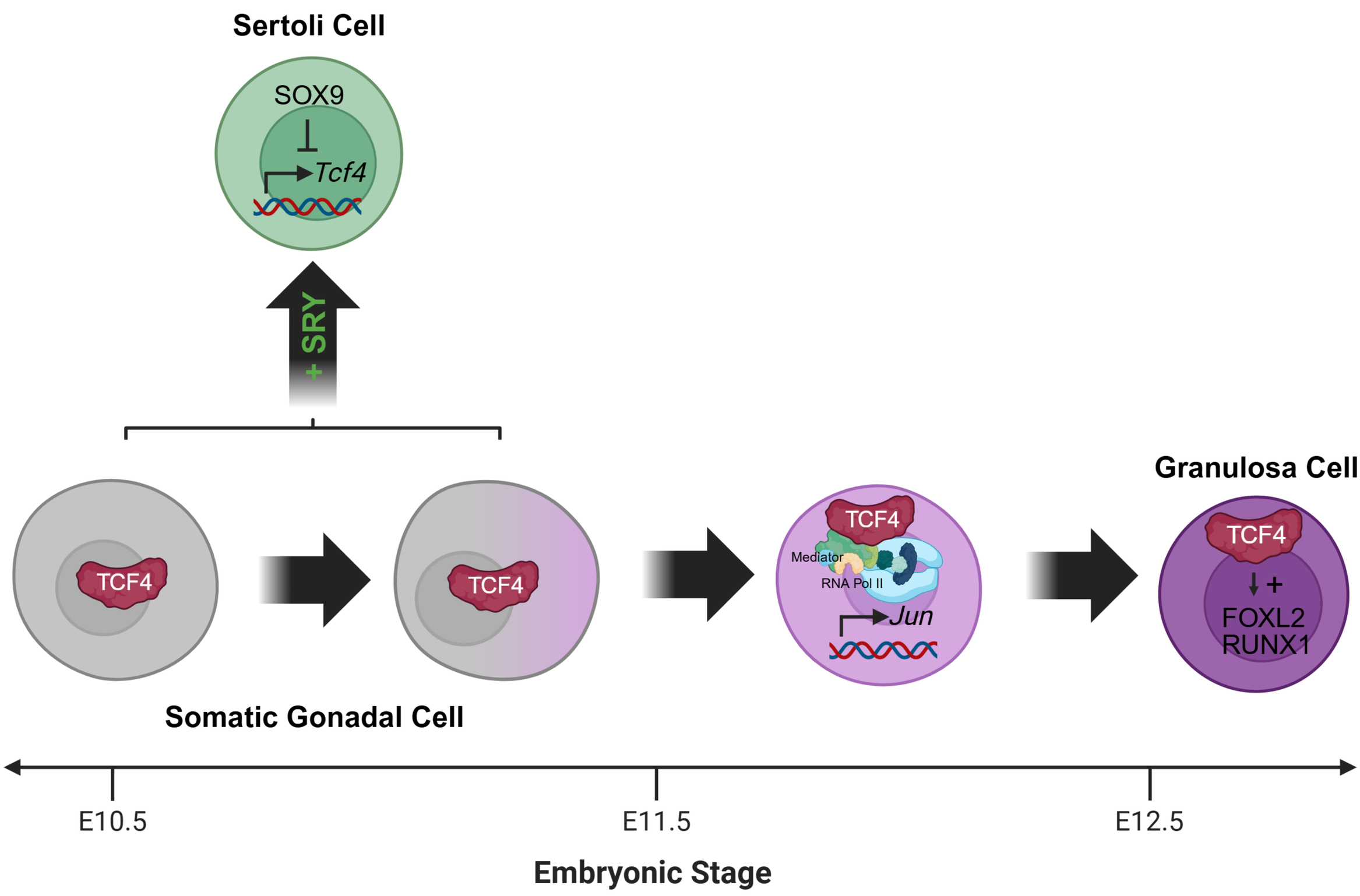
Sertoli Cell
SOX9
Tcf4
+ SRY
TCF4
TCF4
TCF4
Mediator
RNA Pol II
Jun
Granulosa Cell
TCF4
+
FOXL2
RUNX1
Somatic Gonadal Cell
E10.5
E11.5
E12.5
Embryonic Stage